https://doi.org/10.5194/egusphere-2026-3271
Preprint. Discussion started: 14 August 2026

Transport of anthropogenic CH_2Cl_2-rich air from Asia across the North Pacific

Wolfgang Woiwode[1], Bärbel Vogel[2], Valentin Lauther[3], Jens-Uwe Grooß[2], Jeremy Harrison[4,5], Sören Johansson[1], Jörn Ungermann[2], Peter Braesicke[1], Markus Dick[6], Andreas Engel[7], Felix Friedl-Vallon[1], Norbert Glatthor[1], Thomas Gulde[1], Michael Höpfner[1], Markus Jesswein[7,a], Jan Kaumanns[2], Timo Keber[7], Anne Kleinert[1], Erik Kretschmer[1], Guido Maucher[1], Tom Neubert[6], Hans Nordmeyer[1], Christof Piesch[1], Felix Plöger[2,3], Peter Preusse[2], Markus Retzlaff[2], Sebastian Rhode[2], Heinz Rongen[6], Georg Schardt[6], Tanja Schuck[7,b], Björn-Martin Sinnhuber[1], Johannes Strobel[3], Franziska Trinkl[1,c], Ronja Van Luijt[3], Stefan Versick[1], C. Michael Volk[3], Gerald Wetzel[1], Peter Hoor[8], and Martin Riese[2,3]

[1]Institute of Meteorology and Climate Research - Atmospheric Trace Gases and Remote Sensing (IMKASF), Karlsruhe Institute of Technology, Karlsruhe, Germany
[2]Institute of Climate and Energy Systems, Stratosphere (ICE-4), Forschungszentrum Jülich, Jülich, Germany
[3]Institute for Atmospheric and Environmental Research, University of Wuppertal, Wuppertal, Germany
[4]National Centre for Earth Observation, University of Leicester, Leicester, UK
[5]School of Physics and Astronomy, University of Leicester, Leicester, UK
[6]Institute of Technology and Engineering (ITE), Forschungszentrum Jülich, Jülich, Germany
[7]Institute for Atmospheric and Environmental Sciences, Goethe University of Frankfurt, Frankfurt, Germany
[8]Johannes Gutenberg University of Mainz, Institute for Atmospheric Physics, Mainz, Germany
[a]now at: Cooperative Institute for Research in Environmental Sciences, University of Colorado-Boulder, Boulder, CO, USA / NOAA Earth System Research Laboratory Global Monitoring Division, Boulder, CO, USA
[b]now at: Centre for Isotope Research, University of Groningen, Groningen, the Netherlands
[c]now at: Institute for Atmospheric and Environmental Sciences, Goethe University of Frankfurt, Frankfurt, Germany

Correspondence to: Wolfgang Woiwode (wolfgang.woiwode@kit.edu)

Abstract. Dichloromethane (CH_2Cl_2) is emitted mainly anthropogenically and suspected to delay stratospheric ozone recovery. We present in detail the first retrievals of mesoscale 2D distributions of CH_2Cl_2 from infrared limb observations. The airborne remote sensing instrument GLORIA-AB (Gimballed Limb Observer for Radiance Imaging of the Atmosphere, hereinafter "GLORIA") was deployed aboard the German research aircraft HALO during the PHILEAS campaign in August and September 2023 to study the outflow of the Asian Summer Monsoon (ASM). During long-range flights from Alaska, GLORIA observed filaments with elevated CH_2Cl_2 above the North Pacific, Canada and Alaska. Filaments with horizontal extents along the flight track of up to ~1000 km and CH_2Cl_2 volume mixing ratios of locally up to ~400 pptv were observed in the free troposphere, corresponding to levels more than six times higher than the northern hemispheric background for that season. Moderate CH_2Cl_2 enhancements were detected locally also in air masses with characteristics of the extra-tropical lowermost stratosphere. We applied new high-resolution CH_2Cl_2 spectroscopic data, resulting in ~11 % lower volume mixing ratios than in previous analyses using commonly available absorption cross sections. The GLORIA measurements are consistent with in situ observations on HALO by HAGAR-V and GhOST. Using back-trajectory analysis and surface-origin tracers by the CLaMS model, observed filaments are traced back to the ASM region and potential source regions are identified.

https://doi.org/10.5194/egusphere-2026-3271
Preprint. Discussion started: 14 August 2026

Mesoscale filaments are shown to rapidly transport substantial amounts of CH_2Cl_2 from the ASM across the North Pacific into the Northern Hemisphere Upper Troposphere and Lower Stratosphere (UTLS).

1 Introduction

Dichloromethane (CH_2Cl_2), also known as methylene chloride, is a colourless, volatile liquid with a boiling point of ~40°C and vapour pressure of ~470 hPa at 20°C (Ganeff and Jungers, 1948; Thermodynamics Research Center, 2025, and references therein). CH_2Cl_2 is the most abundant chlorinated very short-lived halogenated substance (Cl-VSLS) in the atmosphere and is the main driver that can delay the decline of total inorganic stratospheric chlorine (Cl_y), which plays a critical role in stratospheric ozone depletion (Hossaini et al., 2015; Dubé et al., 2025 and references therein). CH_2Cl_2 is emitted mainly anthropogenically and used in large quantities as solvent and feedstock in industry, particularly for paint removal, chemical synthesis, foam production, and hydrofluorocarbon (HFC) production. High emissions of CH_2Cl_2 in China were attributed to its application as emissive solvent and in the polyurethane foam sector, pharmaceutical use, production leakage and feedstock (Feng et al., 2018, and references therein). Further applications of CH_2Cl_2 include its use in the food sector, for example as solvent for decaffeination of coffee (e.g. Vasquez, 2024).

CH_2Cl_2 is a relatively long-lived Cl-VSLS with an atmospheric lifetime of ~6 months (Engel et al., 2018, and references therein). Its emissions are not controlled by the Montreal Protocol on substances that deplete the ozone layer and its amendments and adjustments, which regulates the use of chlorinated species with the potential to deplete stratospheric ozone. In the last two decades, tropospheric CH_2Cl_2 mixing ratios have been rising considerably (see Advanced Global Atmospheric Gases Experiment (AGAGE), https://www-air.larc.nasa.gov/missions/agage/static/figures/monthly/pdf/CH2Cl2_mm.pdf; accessed on 25 March 2026). By analyzing atmospheric observations and simulations, Hossaini et al. (2017) found indications for an increasing threat from CH_2Cl_2 to stratospheric ozone and that a return of Antarctic stratospheric ozone to levels prior to 1980 could be delayed substantially. Furthermore, Oram et al. (2017) pointed at a growing threat to the ozone layer from anthropogenic Cl-VSLS. They diagnosed an unexplained increase in global tropospheric CH_2Cl_2 abundances by 60 % over the previous decade and a dramatic increase of CH_2Cl_2 and further Cl-VSLS in upper tropospheric air in East and South East Asia. Also, they provided further evidence of atmospheric transport from East Asia to the tropical upper troposphere, from where air masses can enter the stratosphere.

Regional and seasonal emissions of Cl-VSLS and their ozone depletion potential were analysed by Claxton et al. (2019, 2020). Their analyses suggest a relatively efficient transport of Cl-VSLS from continental East Asia to the lower stratosphere and underline the need for denser observations. New concerns with regard to industrial release of VSLS and particularly CH_2Cl_2 were reported by Chipperfield et al. (2020). They pointed out that transport processes, which are not well understood, determine how these species reach the stratosphere.

A rapid increase in industrial CH_2Cl_2 emissions from China was reported by An et al. (2021) based on atmospheric observations. Emissions, primarily from eastern China, increased between 2011 and 2019 at an average rate of ~13% per year,

https://doi.org/10.5194/egusphere-2026-3271
Preprint. Discussion started: 14 August 2026

with the total rise of emissions from China estimated to be comparable in magnitude to the global emission increase over the same period. Assuming that emissions remain at the 2019 levels, a potential delay in Antarctic ozone recovery of ~5 years was projected compared to a scenario with no CH_2Cl_2 emissions. They furthermore pointed out that emissions in Asia have the potential to enter the stratosphere more quickly than emissions from other parts of the world due to the Asian Monsoon circulation and that a continued or expanded monitoring of CH_2Cl_2 and other VSLS is required.

The Asian Summer Monsoon (ASM) links local emission sources with the large-scale circulation (e.g. Mason and Anderson, 1963; Li et al., 2005; Riese et al., 2025). The continental ASM comprises the South Asian Summer Monsoon and the East Asian Summer Monsoon. In the vertical domain, the ASM can be roughly subdivided into two components: a low-level cyclonic circulation together with a strong convective part below ~12 km, and above, the Asian Summer Monsoon Anticyclone (ASMA), a dynamically coupled upper-level anticyclonic flow that reaches up to ~18 km. The ASMA stretches across a large fraction of Asia and is linked to the subtropical jet stream (e.g. Park et al., 2007). The anticyclone edge acts as a transport barrier (e.g. Ploeger et al., 2015). Transport pathways out of the ASM region exist at both altitude regimes (e.g. Dunkerton, 1995; Santee et al., 2017; Clemens et al., 2022). At regions of the low-level cyclonic flow, eastward transport across the Pacific along the subtropical jet stream and stripping of filaments take place at tropospheric levels. At the levels of the ASMA two main pathways were discussed by Ploeger et al. (2017). One main pathway is direct transport into the tropical pipe. The other main pathway is quasi-horizontal isentropic stripping of filaments into the extratropical stratosphere at levels around ~380 K. Quantification of their relative relevance and year-to-year variability remains challenging.

Observations of elevated CH_2Cl_2 mixing ratios in and above the ASM by means of airborne observations from Nepal in 2017 were reported by Adcock et al. (2021). Their findings show that the ASMA transports larger quantities of Cl-VSLS to the UTLS than expected. Efficient pathways for Cl-VSLS via the Asian and North American Monsoon into the lowermost stratosphere (LMS) were analysed by Lauther et al. (2022) by using airborne in situ observations of CH_2Cl_2 and $CHCl_3$ above the Northern Atlantic Ocean and Western Europe. Using Lagrangian back-trajectories, they derived two pathways from (sub)tropical source regions into the extratropical upper troposphere and lower stratosphere (UTLS) in northern hemisphere late summer. One pathway includes convective uplift to high tropospheric levels followed by further upwelling in the ASMA in summer and subsequent eastward-outbreak from the anticyclone. Another pathway into the extratropical LMS was derived from low mixing ratios of the same species. It involved different uplift mechanisms, followed by fast transport in the extratropical transition layer (ExTL) and free troposphere, and by quasi-isentropical transition into the extratropical LMS. Aircraft observations by Smith et al. (2024) in the North American troposphere and LMS documented that CH_2Cl_2 increased over the past two decades at all levels throughout the troposphere, and to a weaker degree, also in the stratosphere. They stress the urgency of investigating CH_2Cl_2 sources and that CH_2Cl_2 trends in the lower stratosphere should be monitored closely.

Record-breaking mixing ratios of CH_2Cl_2 at the base of the stratosphere were reported by Pan et al. (2024) over the western Pacific in the outflow of the East Asian Monsoon during the ACCLIP (Asian summer monsoon Chemical and Climate Impact Project) by means of aircraft observations in 2022 close to the ASM region. They conclude that deep convection in the ASM constitutes a significant process lifting pollutants from the planetary boundary layer to the tropopause, thus enabling injection

https://doi.org/10.5194/egusphere-2026-3271
Preprint. Discussion started: 14 August 2026

into the stratosphere. Their results suggest that a reevaluation of the contribution of Cl-VSLS via the ASM to the total stratospheric chlorine budget is warranted. Using airborne observations from Alaska in 2023, Jesswein et al. (2025) traced elevated abundances of CH_2Cl_2 in the subarctic upper troposphere to the ASM. They detected enhanced CH_2Cl_2 volume mixing ratios in the upper troposphere and tropopause region and projected only a minor potential of the observed air masses to reach the stratosphere. Currently, it is unclear to which degree CH_2Cl_2 is capable of reaching the stratosphere and affecting the ozone layer (cf. e.g. Adcock et al., 2021; Lauther et al. 2022; Pan et al., 2024; Jesswein et al., 2025, Laube et al., 2025, Vogel et al., 2026). The need for an improvement of measurement networks and systems to observe VSLS is pointed out also by Saiz-Lopez et al. (2025).

The campaign "Probing High Latitude Export of Air from the Asian Summer Monsoon" (PHILEAS) addressed the current gap in observations in the northern hemisphere transition area at tropospheric and lower stratospheric levels (Riese et al., 2025). Using airborne observations aboard the German research aircraft HALO (High Altitude and LOng Range Research Aircraft) from Oberpfaffenhofen, Germany, and Anchorage, Alaska, in combination with atmospheric models, PHILEAS investigated the outflow of the ASM in summer and early autumn 2023 at tropospheric and lower stratospheric levels.

The Gimballed Limb Observer for Radiance Imaging of the Atmosphere (GLORIA) was part of the scientific payload of HALO during PHILEAS. GLORIA is an infrared limb-imager designed for application aboard high-altitude aircraft and stratospheric balloon and a demonstrator for potential future satellite missions (Friedl-Vallon et al., 2014; Riese et al., 2014; Wetzel et al. 2025). It has been deployed successfully in numerous airborne campaigns aboard high-altitude research aircraft and stratospheric balloon to study atmospheric composition and dynamics (e.g. Höpfner et al., 2019; Johansson et al., 2022; Krasauskas et al, 2021; Geldenhuys et al., 2023).

Here, we present in detail the first 2D infrared limb observations of mesoscale CH_2Cl_2 distributions by GLORIA above the North Pacific, Canada and Alaska during PHILEAS and involving new unpublished spectroscopic absorption cross sections by Harrison (in preparation). Together with in situ observations and Lagrangian transport simulations, we analyse CH_2Cl_2-rich filaments and their transport across the North Pacific. Thereby, we address the following research questions:

1. What are typical sizes and volume mixing ratios of CH_2Cl_2-rich filaments observed in the outflow of the ASM 2023?
2. At which levels are the filaments located within the UTLS?
3. What are the transport pathways and where are possible source regions?

In the focus of our study are research flights that were analysed previously by Jesswein et al. (2025) by means of in situ observations. The GLORIA observations extend the in situ observations to a mesoscale 2-dimensional perspective and provide new information on vertical and horizontal extent and structures of these filaments in the UTLS. Using Lagrangian back-trajectories and surface-origin tracers, we analyse transport pathways of the filaments and identify potential source regions.

In section 2 we introduce the PHILEAS campaign, GLORIA observations, new spectroscopic data, co-located in situ observations and model data. In section 3, mesoscale CH_2Cl_2-rich filaments above the North Pacific, Canada and Alaska that were observed during three selected flights are analysed. In section 4, GLORIA observations of a flight on 26 and 27 August 2023 are compared with co-located in situ observations. In section 5, potential source regions of the observed filaments are analysed by means of Lagrangian back-trajectories. For a flight on 16 and 17 September 2023, where the highest CH_2Cl_2 mixing ratios were observed, we use surface-origin tracers to gain further insights with regard to potential source regions. The results are summarised and discussed in section 6.

2 Methods

2.1 PHILEAS campaign

An overview of the PHILEAS campaign is provided by Riese et al. (2025). PHILEAS aimed at investigating (i) the evolution of gaseous and particulate species in large-scale filaments shed from the ASMA, (ii) main transport pathways and timescales of pollutants from the ASM region into the UTLS and (iii) the large-scale impact of the ASMA on the extratropical stratosphere. For this purpose, 20 research flights were conducted by the German research aircraft HALO in three campaign phases from Oberpfaffenhofen (Germany) and Anchorage (Alaska) in August and September 2023. HALO is capable of long-range research flights across distances larger than 9000 km and ceiling altitudes of up to ~15 km. As discussed by Riese et al. (2025), the climatological signature of the ASMA in summer 2023 was characterised by (i) a slightly elevated tracer anomaly in the center of the East Asian component and (ii) above-average flushing of the lowermost stratosphere, thus providing suitable conditions to study potential CH_2Cl_2 signatures in the UTLS.
The goal of the main phase in Anchorage from 21 August 2023 to 19 September 2023 was to investigate eastward transport of moist and polluted air masses across the Pacific and their mixing into the lowermost stratosphere (LMS). Flight planning involved forecasts by the Chemical Lagrangian Model of the Stratosphere (CLaMS, McKenna, 2002a,b; Pommrich et al., 2014, and references therein), the ICON-ART model (ICOsahedral Nonhydrostatic with the extension Aerosols and Reactive Trace gases, Schröter et al., 2018, and references therein), the ECMWF (European Centre for Medium-Range Weather Forecasts) IFS (Integrated Forecast System) and the ECMWF CAMS (Copernicus Atmosphere Monitoring Service). Here, we focus on selected flights during the main campaign phase, which targeted large filaments with high fractions of air from the ASM region and where the most pronounced CH_2Cl_2-rich filaments were detected by GLORIA. In situ observations of CH_2Cl_2 during these flights and an analysis of the transport pathways of the probed air masses at flight level from the ASM region were reported by Jesswein et al. (2025) and Vogel et al. (2026).

2.2 GLORIA observations

GLORIA is a limb-imaging Fourier transform infrared spectrometer designed for stratospheric research aircraft and balloon (Friedl-Vallon et al., 2014; Riese et al., 2014; Wetzel et al. 2025). The instrument involves a Michelson interferometer, which is coupled to an HgCdTe imaging detector array. In the aircraft version, the spectrometer is housed in a gimballed frame for stabilisation of the line-of-sight and azimuth panning. In the configuration used during PHILEAS, 128 vertical times 48

https://doi.org/10.5194/egusphere-2026-3271
Preprint. Discussion started: 14 August 2026

horizontal pixels of the detector were used for simultaneous limb observations from ∼5 km up to the flight altitude and limited upward sampling. Each GLORIA observation represents a data cube consisting of all interferograms which are recorded by the individual pixels simultaneously. In the data processing, the interferograms are transformed into spectra. The spectra of the detector rows are averaged to superpixels, forming one vertical column of 128 measurements per observation.

In the airborne configuration, the viewing direction is to the right-hand side of the flight track and the azimuth direction can be panned. Different measurement modes can be applied for GLORIA, which represent trade-offs between spectral sampling density and horizontal along-track sampling. For the CH_2Cl_2 retrieval, we use GLORIA high spectral resolution mode observations. This measurement mode is characterised by a high spectral sampling of 0.0625 cm^{-1} and a sampling frequency of one limb image every ~3 km (e.g., Johansson et al., 2018). Also possible are measurements with a lower spectral resolution and a high sampling frequency, which enables tomography (e.g. Krasauskas et al., 2021). From each observation, a set of 128 calibrated spectra results (Fig 1a). The observations cover a spectral range from ~750 cm^{-1} to 1450 cm^{-1} and include spectral signatures of CO_2, O_3, H_2O, chlorofluorocarbons (CFCs), hydrocarbons, and many other minor species. Instrumental gain and offset uncertainties are estimated within 1 % and 30 nW cm^{-2} sr^{-1} cm, respectively (Ungermann et al., 2022).

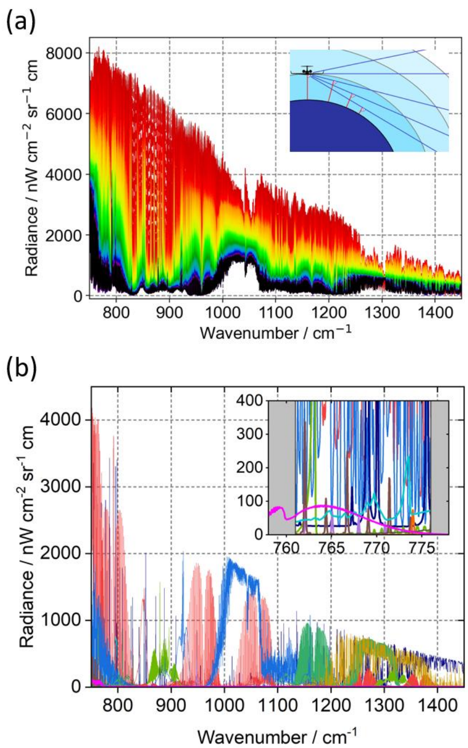

Figure 1. Observed and synthetic spectra. (a) Calibrated spectra with different vertical viewing angles (colour-coded) resulting from a single GLORIA observation during PHILEAS research flight F17. Observed radiances increase with decreasing tangent altitude. (b) Synthetic spectra of individual contributions by different trace gases for a GLORIA observation calculated for a flight altitude of 13 km and a tangent altitude of 8 km and assuming a vertically constant CH_2Cl_2 volume mixing ratio of 100 pptv in the troposphere. The inset shows a close-up of the spectral microwindow used for the CH_2Cl_2 retrieval. Signatures by CH_2Cl_2 and interfering gases are shown in magenta (CH_2Cl_2), red (CO_2), blue (O_3), dark blue (H_2O), cyan (CCl_4), green (HNO_3), brown (C_2H_2), light pink (HCN) and orange (COF_2).

https://doi.org/10.5194/egusphere-2026-3271
Preprint. Discussion started: 14 August 2026

2.2 CH_2Cl_2 absorption cross sections

The infrared spectroscopy of CH_2Cl_2 is discussed by Shimanouchi and Suzuki (1962) and Wallington et al. (2016). For the retrieval of CH_2Cl_2 from the GLORIA observations, we use a spectral microwindow in the region of the υ_9 band, which is centred at ~760 cm^{-1} (Fig. 1b). For the previous retrieval setup reported in Riese et al (2025), we used absorption cross sections by Sharpe et al. (2004), which are available via the HITRAN website (Gordon et al., 2022). These are N_2-broadened composite cross sections derived from measurements at 0.1125 cm^{-1} spectral resolution, over a range of mixing ratios at 760 Torr (1013 hPa), and 278, 298, and 323 K. Due to these relatively high temperatures and pressures, these absorption cross sections are not very representative of the conditions of the GLORIA observations in the UTLS.

This work, therefore, makes use of new absorption cross sections by Harrison (in preparation), based on spectra recorded at a high spectral resolution of 0.015 cm^{-1}, covering a temperature range of 198 K to 295 K and a pressure range of 50 Torr to 760 Torr (67 hPa to 1013 hPa). These absorption cross sections are well suited for the atmospheric conditions during the GLORIA observations. Using these new absorption cross sections, we now retrieved ~11 % lower volume mixing ratios from the GLORIA observations when compared to our previous data product which was used by Riese et al. (2025) and Trinkl (2025) (see Appendix A).

2.2 CH_2Cl_2 retrieval from GLORIA observations

The retrieval of temperature, trace gases and cloud parameters in GLORIA high spectral resolution mode observations is done by calculation of synthetic spectra (Stiller et al., 2002 and references therein) and inversion (Höpfner et al., 2001 and references therein). Details of the GLORIA retrieval are described by Johansson et al. (2018, 2022 and references therein). For the retrieval of CH_2Cl_2, we use the spectral microwindow from 761.0 cm^{-1} to 776.0 cm^{-1} in the υ_9 band region of CH_2Cl_2 (Fig. 1b). In this spectral region, CH_2Cl_2 signatures are relatively strong and sufficiently separable from signatures by interfering species. The observations are filtered according to the cloud index by Spang et al. (2004) with a conservative threshold value of 5. Retrieval parameters are the volume mixing ratios of CH_2Cl_2, the interfering species H_2O, O_3, HNO_3, HCN, C_2H_2, and CCl_4, temperature, a wave number-independent background continuum and spectral shift. A vertically constant profile with approximately zero (10^{-2} pptv) CH_2Cl_2 is used as initial guess and a priori profile. We furthermore mention that $ClONO_2$ is another species which can significantly affect the CH_2Cl_2-retrieval in this microwindow in higher latitude and/or altitude ranges, particularly in polar winter.

The retrieved vertical profiles are characterised by a median vertical resolution of ~750 m and a median combined random and systematic 1σ uncertainty of ~30 % (Figure 2). The retrieval uncertainties were calculated according to Johansson et al. (2018). Here, the following 1σ uncertainties were taken into account: spectroscopic uncertainties for CH_2Cl_2 (3%), vertical pointing uncertainties (0.03°), instrument offset uncertainties (30 nW cm^{-2} sr^{-1} cm) and radiometric gain uncertainties (1%). Note that the uncertainties vary partly with altitude and atmospheric scenario. In the graphs shown in the next sections, only data points

https://doi.org/10.5194/egusphere-2026-3271
Preprint. Discussion started: 14 August 2026

with a vertical resolution of better than 1500 m are shown. The vertical profiles of CH_2Cl_2 volume mixing ratios resulting from the individual observations are combined to vertical cross sections along the flight path.

Furthermore, we use GLORIA temperature data to calculate potential temperature as vertical coordinate. The temperature retrieval is done using a similar setup as described by Johansson et al. (2018). It is characterised by a typical vertical resolution of ~500 m and combined total 1σ uncertainties of ~1 K. For calculation of potential temperature, pressure data from the ECMWF analysis are used.

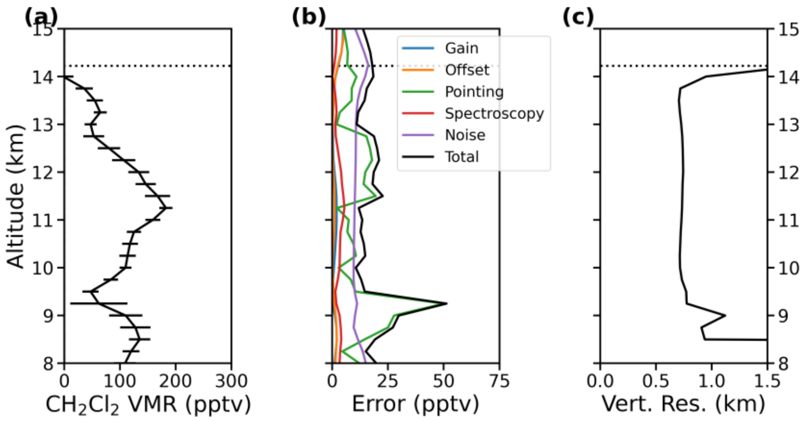

Figure 2. Characteristics of an exemplary retrieved vertical profile of CH_2Cl_2 for PHILEAS research flight F08 on 26 and 27 August 2023 at 23:16 UTC. (a) Volume mixing ratio of CH_2Cl_2 with combined random and systematic total uncertainty (1σ), (b) individual uncertainty contributions and total uncertainty, and (c) vertical resolution. Dotted line marks flight level.

2.3 In situ observations

HAGAR-V and GhOST were deployed on HALO during PHILEAS. Both instruments involve gas chromatography with mass spectrometry (GC-MS) for the detection of CH_2Cl_2 and many other trace species. The setup and characteristics of HAGAR-V and GhOST during PHILEAS are discussed by Jesswein et al. (2025) and references therein. In order to enhance the observation frequency, HAGAR-V was operated using two GC systems which targeted the same species. Thereby, a time resolution of 2 min with a sample integration time of 30 s in combination with an average precision of 1.3 % was achieved. GhOST used one single GC-channel and was operated with a time resolution of 6 min and a sample integration time of 147 s. The average precision of the GhOST CH_2Cl_2 measurements during PHILEAS is 0.9%. GhOST used one and HAGAR-V two inflight calibration gases. The evaluation of the measurements is based on AGAGE-derived calibrations (SIO-14, Prinn et al., 2018 and references therein). Further information on a previous setup of HAGAR-V can be found in Lauther et al. (2022). Further information on GhOST can be found in Keber et al. (2020) and Jesswein et al. (2021).

Note that CH_2Cl_2 abundances are determined by both instruments referring to a gravimetric approach and are expressed in parts per trillion (ppt), while from the GLORIA observations, CH_2Cl_2 abundances are retrieved in parts per trillion by volume

https://doi.org/10.5194/egusphere-2026-3271
Preprint. Discussion started: 14 August 2026

(pptv). Within the pressure range of the observations and the uncertainties of the comparisons shown here, differences between these quantities are negligible and, in the following, we will use the unit pptv also for the in situ observations.

2.4 CLaMS simulations

To investigate the origin of mesoscale filaments observed by GLORIA, the Chemical Lagrangian Model of the Stratosphere CLaMS (McKenna, 2002; Pommrich et al., 2014; references therein) is applied. We use a 3-dimensional CLaMS simulation including surface-origin tracer as well as pure CLaMS back-trajectory calculations as decribed in Vogel et al. (2026). Both 3-dimensional CLaMS simulations as well as the back-trajectory calculations are driven by ECMWF ERA5 reanalysis data (Hersbach et al., 2020 and references therein) with a horizontal resolution of 0.3° × 0.3°. ERA5 data are directly provided by the ECMWF on a 0.3° × 0.3° horizontal grid and are characterised by 137 vertical levels up to 0.01 hPa and a time resolution of 1 h.

Vertical transport plays an important role in the evolution of the observed filaments. In CLaMS, the diabatic approach is used to calculate vertical velocities. Potential temperature is applied as the vertical coordinate at pressures less than approximately 300 hPa, i.e. in the UTLS. Here, the vertical velocity is determined solely by the total diabatic heating rate from ERA5 reanalysis (Pommrich et al., 2014; Ploeger et al., 2021). However, in the first layers below the reference level, the vertical coordinate is also still close to diabatic as the transition from potential temperature to an orography-following vertical coordinate occurs rather slowly (e.g. Pommrich et al., 2014). Therefore, the vertical velocity includes information on convective transport as resolved in the reanalysis vertical wind and total diabatic heating rate (see Pommrich et al., 2014). In the applied CLaMS simulations, convection is driven only by the ERA5 reanalysis.

Diabatic back-trajectories are calculated using the CLaMS trajectory module (e.g. Vogel et al., 2024, 2026 and references therein). The back-trajectories are calculated using the ERA5 data at a 0.3° × 0.3° horizontal grid and outputs are generated hourly. At their first intersection with the model boundary layer, which is defined as 2–3 km above the orography-following model surface, back-trajectories are terminated. The back-trajectories are analysed over a period of 14 days.

We involve 3-dimensional CLaMS simulations using surface-origin tracers (e.g. Vogel et al., 2015) to trace back potential source regions of CH_2Cl_2-rich air masses. In our study, a tracer setup for the surface-origin tracers is used as described in Vogel et al. (2026). The simulation starts on 1 May 2023 and covers the entire ASM season 2023. Surface-origin traces are released in the boundary layer (i.e. ~2-3 km above ground level) under consideration of orography in the defined regions. The surface-origin tracers are set to 1 in the corresponding region every 24 hours and are then transported and mixed into the free atmosphere. Discrete mixing steps are simulated every 24 hours. Here, we use the surface-origin tracers from the regions Northern Western Pacific (NWP), Tropical Western Pacific (TWP), Eastern China (ECH), Southeast Asia (SEA), Tibetan Plateau (TIB), Bay of Bengal (BoB), Northern Indian Subcontinent (NIN), Indian Subcontinent (IND), and Northern Indian Ocean (NIO). The regions are visualised in section 5.3.

https://doi.org/10.5194/egusphere-2026-3271
Preprint. Discussion started: 14 August 2026

3 Observations of mesoscale CH_2Cl_2 filaments

Prominent CH_2Cl_2-rich filaments were observed on flights in August and September 2023 during the main phase of PHILEAS based in Alaska. During these flights, Jesswein et al. (2025) detected CH_2Cl_2 abundances of up to 300 pptv in situ at flight level. The GLORIA observations presented here extend these observations to a 2D perspective and show filaments below the flight altitude. By plotting the vertical profiles derived from the GLORIA observations against the distance along flight route (see "Distance" coordinate in the following Figures), we furthermore infer the approximate extent along flight tracks.

PHILEAS research flight F08 on 26 to 27 August probed filaments with high fractions of air originating from South Asia. As discussed by Riese et al., (2025), the air masses were transported across the Pacific during a strong Rossby wave breaking event that occurred during the previous four days. Tropospheric air was directed to the North along the Aleutian trough and then along a southward cyclonic flow (see Riese et al. 2025, Fig. 8). Wave breaking resulted in further filamentation and subsequent mixing. During this flight, a tropospheric CH_2Cl_2-rich filament stretching across the eastern part of the Gulf of Alaska was observed by GLORIA (Fig. 3a, b). CH_2Cl_2 levels peaking at ~300 pptv were detected locally. The filament contained mesoscale fine structures, suggesting that filamentation and mixing of substructures with higher CH_2Cl_2 loadings was in progress. The horizontal extension of the filament along the flight track was ~700 km. Further diffuse filamentary structures with up to ~150 pptv CH_2Cl_2 were detected in the troposphere directly after waypoint III before the main filament was detected. Note that the long light paths of the limb-views make the observations sensitive to chemical species with low abundances, such as CH_2Cl_2. However, it results in significant horizontal averaging along the line-of-sight and an increasing horizontal distance of the measurement location for decreasing tangent altitudes (see Inset in Fig. 3b). During this flight, CH_2Cl_2 data is only available after waypoint III, since the first part of the flight was optimised for in-situ measurements and, at the same time, a different GLORIA measurement mode was applied. Missing data points in the lower parts of the shown profiles correspond to cloud-affected regions, which are not transparent in the infrared.

To differentiate between air masses with tropospheric and stratospheric character, the 2 PVU, 4 PVU and 8 PVU isolines were interpolated from the ECMWF analysis and are superimposed in Fig. 3a. The 4 PVU isoline can be regarded as conservative proxy for the dynamical tropopause (cf. Bauchinger et al., 2025). Above the 4 PVU-tropopause, diffuse filamentary structures with enhanced CH_2Cl_2 were detected along the distance coordinate at 3700 km to 3800 km and after 4600 km. In the latter case, a deformation in the 4 PVU and 8 PVU isolines indicates a dynamical distortion of the tropopause region, probably fostering filamentation and mixing. In the centre of the structure, observed CH_2Cl_2 abundances peaked locally at ~125 pptv and reached into air masses with LMS character until 5600 km. In the westward-looking section after waypoint IV, again CH_2Cl_2 levels exceeding 100 pptv were observed in air masses with LMS character, which probably belonged to the same filament which was detected before by GLORIA at around 5000 km (compare distribution of tangent points in Fig. 3b).

https://doi.org/10.5194/egusphere-2026-3271
Preprint. Discussion started: 14 August 2026

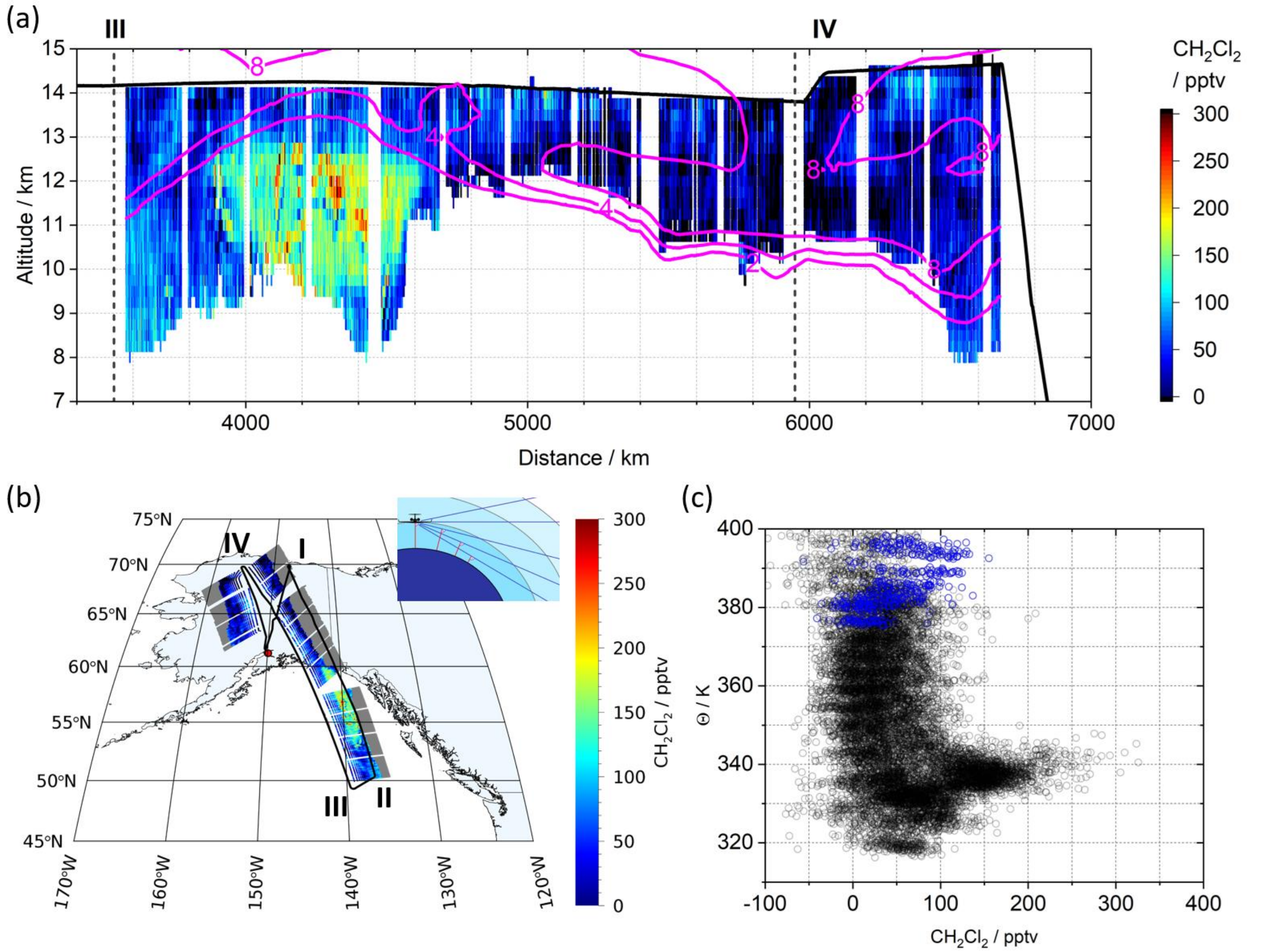

Figure 3. Mesoscale structures of CH_2Cl_2-rich filaments above the North Pacific and Alaska as observed by GLORIA during PHILEAS research flight F08 on 26 and 27 August 2023. (a) Vertical cross section of retrieved CH_2Cl_2 volume mixing ratios (colour-coded) along flight track. Pink solid lines indicate potential vorticity isolines interpolated from the ECMWF analysis. (b) GLORIA observations in the horizontal domain. Retrieved CH_2Cl_2 volume mixing ratios are superimposed on the geolocations of the tangent points. Grey data points indicate cloud-affected observations. Black solid lines in (a,b) indicate the HALO flight track. The inset in (b) visualises the altitude-dependent geometries of the GLORIA limb views and tangent points schematically (from Woiwode et al. (2018)). (c) Vertical distribution of retrieved CH_2Cl_2 volume mixing ratios including all data points of the flight. Potential temperature levels were calculated from GLORIA temperature data and pressure data from the ECMWF analysis. The data points highlighted in blue correspond to the section of the diffuse filament along the distance coordinate after waypoint IV between 6250 km and 6450 km at altitudes >12.5 km.

A profile of all GLORIA CH_2Cl_2 data points of research flight F08 versus potential temperature is shown in Figure 3c. CH_2Cl_2 levels of the main filament peaking at ~300 pptv correspond to potential temperature levels around 340 K. Elevated volume mixing ratios are found mainly between about 320 K and 350 K which confirms the tropospheric character. Above and below, the data points are mostly scattered around background levels of ~50 pptv or lower. Data points slightly scattering to higher volume mixing ratios are also found between 380 K and 400 K. They correspond with the diffuse maxima above the dynamical

https://doi.org/10.5194/egusphere-2026-3271
Preprint. Discussion started: 14 August 2026

tropopause (Fig. 3a,b) and strongly suggest that these structures are located in the LMS (cf. Holton et al., 1995). Datapoints corresponding to the diffuse filament at the end of the flight are highlighted in blue in Fig. 3c for identification.

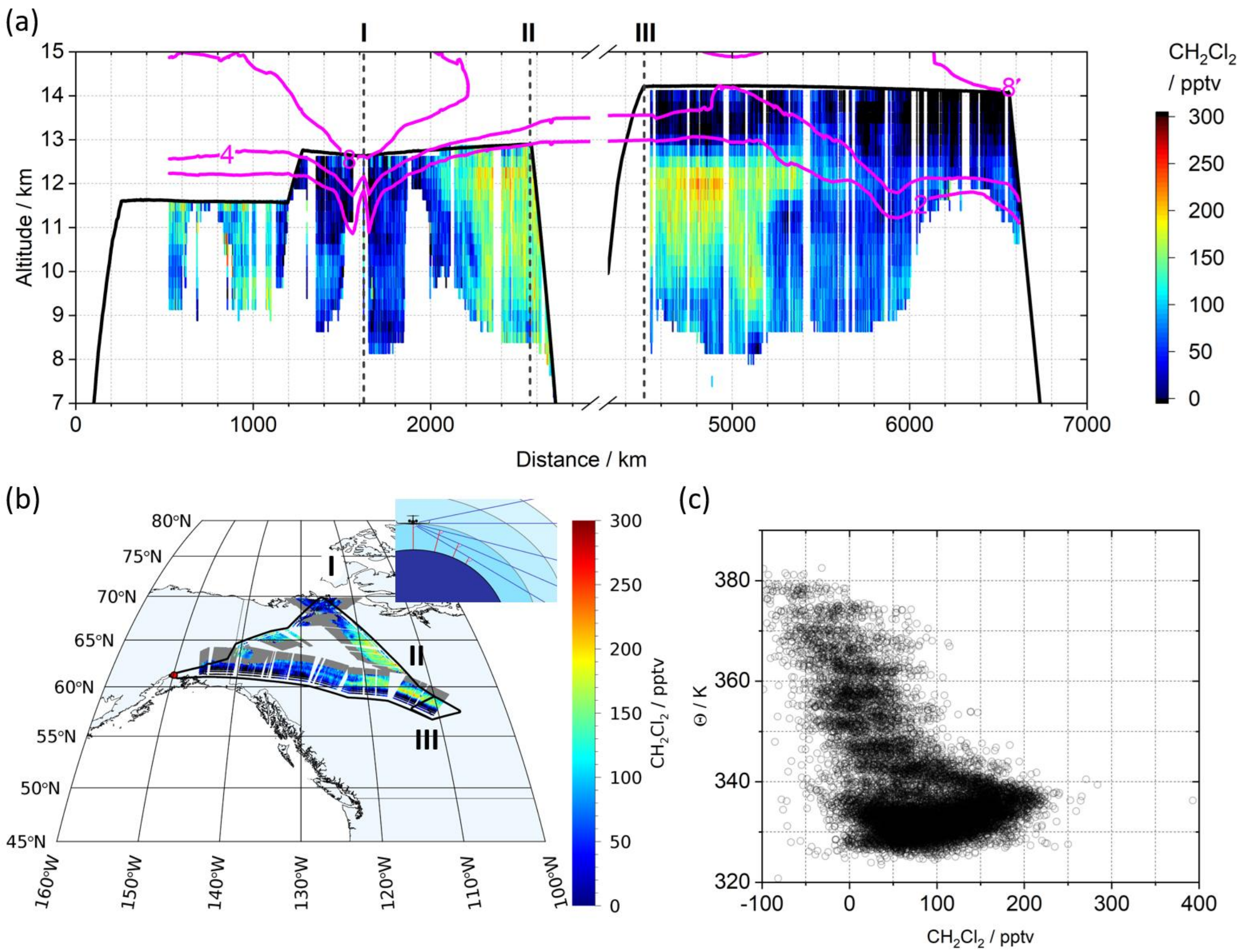

Figure 4. Wide-ranging CH_2Cl_2 filaments above Canada as observed by GLORIA during PHILEAS research flight F09 on 28 and 29 August 2023. For plotting details, see Fig. 3.

Wide-ranging filaments with enhanced CH_2Cl_2 levels were detected during PHILEAS research flight F09 on 28 and 29 August 2023 above Alaska and Canada (Fig. 4). The flight was conducted only one day after the previously discussed flight and aimed at revisiting partly the same air masses probed the day before after further dynamical evolution. CH_2Cl_2 maxima with horizontal extensions of more than 600 km along flight track are found prior to waypoints I and II (Fig., 4a,b). A large filament stretching across ~1000 km is detected after waypoint III. CH_2Cl_2 peak values well exceeding 200 pptv are observed in the filaments prior to II and after III. Note that these filaments appear to be connected structures (Fig. 4b) and together constitute an even larger filament. Since the filament is likely to extent further to the Southeast, the extent derived from the GLORIA observations

https://doi.org/10.5194/egusphere-2026-3271
Preprint. Discussion started: 14 August 2026

represents an estimate of its minimum extension. A gap in the GLORIA observations between II and III corresponds with a dedicated flight pattern for in situ observations at lower flight altitudes.

During this flight, only weak indications of CH_2Cl_2 enhancements are detected in the tropopause region (see CH_2Cl_2 volume mixing ratios around 4 PVU isoline in Fig. 4a). The tropospheric character of the observed large filaments is confirmed by the vertical profile shown in Fig 4c. The maxima are located mainly between about 325 K and 350 K. Above ~360 K, CH_2Cl_2 volume mixing ratios detected by GLORIA are scattered mostly around 0 pptv, suggesting that older stratospheric air masses or air masses of tropospheric origin with low CH_2Cl_2 abundances were detected. A pronounced scattering of data points to negative values above 370 K hints at locally enhanced systematic uncertainties in the GLORIA data at these rather low CH_2Cl_2 abundances.

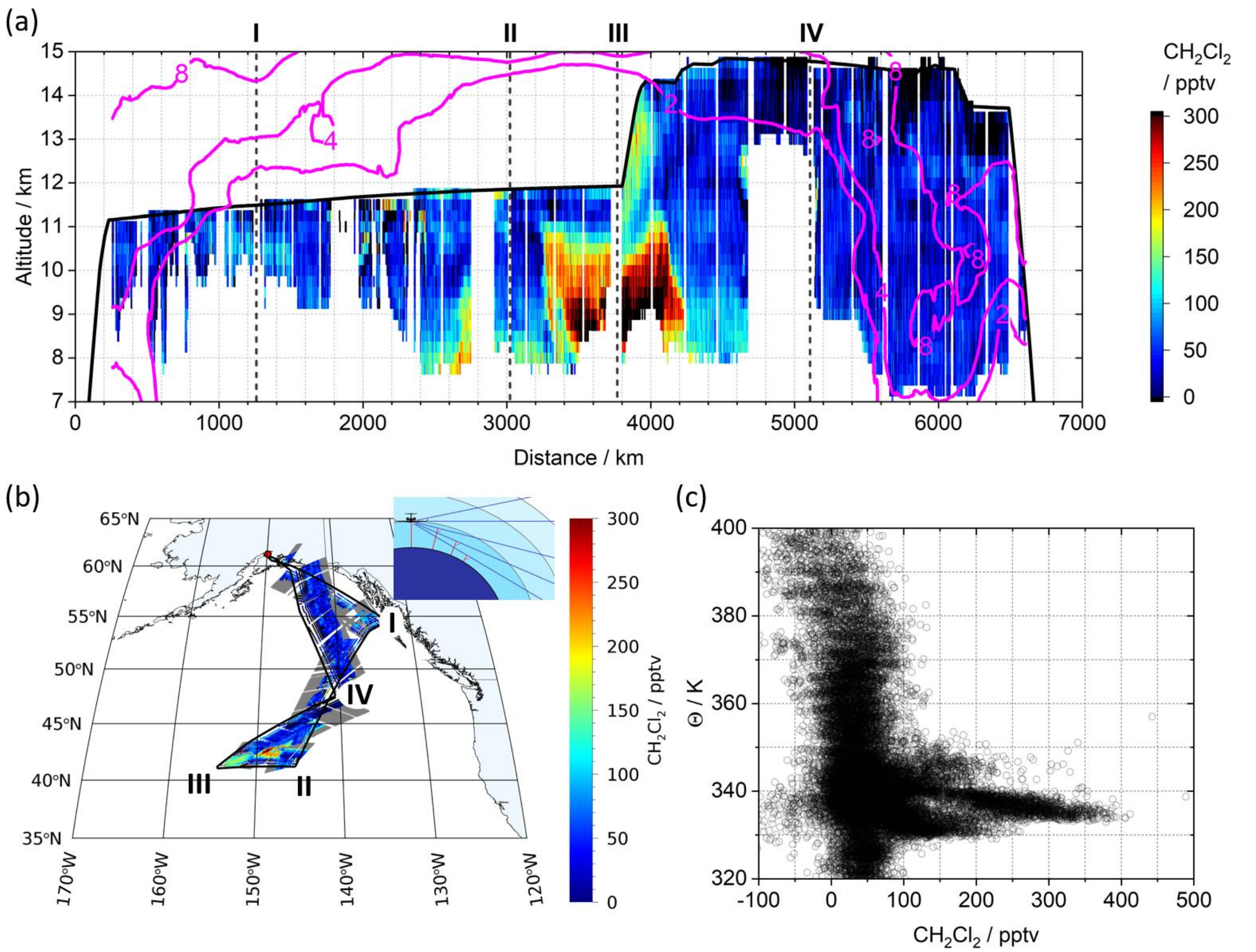

Figure 5. High CH_2Cl_2 levels detected by GLORIA during PHILEAS research flight F17 on 16 and 17 September 2023 above the North Pacific. For plotting details, see Fig. 3.

https://doi.org/10.5194/egusphere-2026-3271
Preprint. Discussion started: 14 August 2026

The highest CH_2Cl_2 abundances were detected by GLORIA during research flight F17 on 16 and 17 September 2023 above the North Pacific. In this phase of the summer, air masses from the ASM region were transported rapidly across the Pacific and subjected to strong shear (Riese et al., 2025). CH_2Cl_2 volume mixing ratios peaking at ~400 pptv were detected by GLORIA below ~11 km around waypoint III (Fig. 5). Around this waypoint, GLORIA observations depict twice approximately the same region (Fig. 5b) and sections of ~400 km of the filament are detected in a northward and south-eastward direction, respectively. During the same flight, Jesswein et al. (2025) reported in situ peak values of CH_2Cl_2 of ~300 ppt. The GLORIA observations show that noticeably higher CH_2Cl_2 levels were present in the same flight section in a separate filament at lower altitudes. At flight altitude, a weaker separate maximum is observed by GLORIA between 3600 km and 4000 km, consistent with Jesswein et al. (2025).

Further weaker filamentary structures with enhanced CH_2Cl_2 levels are found during the other sections of the flight until ~4700 km, illustrating the state of transport and filamentation of CH_2Cl_2-rich air masses above the probed region of the North Pacific in late summer 2023. In the last part of the flight, a broad tropopause fold with lowermost stratospheric potential vorticity levels > 4 PVU reaching below 8 km is seen in Fig. 5a. Only weak indications of enhanced CH_2Cl_2 levels are found in these air masses with LMS character. The vertical distribution in Fig. 5c shows that the filaments seen in Fig. 5a,b are situated in narrow layers between 325 K and 350 K in the free troposphere.

4 Comparison of GLORIA observations with in situ observations

Research flight F08 on 26 and 27 August 2023 provided the opportunity to compare the GLORIA CH_2Cl_2 data with in situ observations by HAGAR-V and GhOST at different levels. The flight pattern was arranged such that the GLORIA observations after waypoint III intersected approximately with the in situ observations at levels around ~12.5 km and 13.5 km, thus providing a close match of the GLORIA remote observations with the in situ observations (Fig. 6a,b, sections A and B). Furthermore, at flight level, a direct comparison with the in situ observations is possible, because the tangent points of the limb observations are relatively close to the flight path (Fig. 6b, section C). Note however that GLORIA limb observations are also affected by the atmospheric scene *normal* to the flight track in front of and behind the tangent point, (e.g. Woiwode et al., 2018). In contrast, the in situ observations, which involve sample collection, represent integrated observations *along* the flight track. This needs to be reminded when comparing the observations and can explain local discrepancies in regions, where strong gradients are present in trace gas distributions.

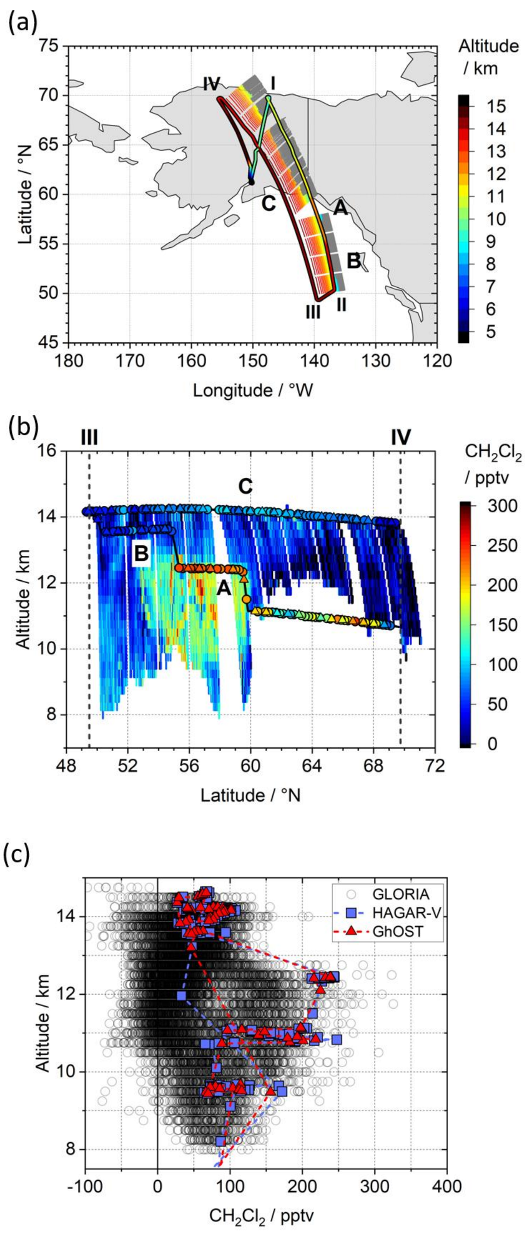

Figure 6. Comparison of GLORIA CH_2Cl_2 data with collocated in situ observations by HAGAR-V and GhOST during research flight F08 on 26 and 27 August 2023. (a) Horizontal distribution of GLORIA tangent points. Tangent altitudes of the data points are colour-coded. Grey data points indicate cloud-affected observations. The colour-coded solid line indicates the flight track and altitude of HALO. Tangent points after IV are not shown for easier comparison with panel (b). (b) Meridional projection of CH_2Cl_2 distribution detected by GLORIA from waypoint III to IV (colour-coded) and approximately matching observations by HAGAR-V and GhOST (colour-coded circles and triangles, respectively) from waypoint I to IV. The black solid line (mostly hidden by datapoints of in situ observations) indicates the flight altitude of HALO. (c) Comparison of all GLORIA data points with all HAGAR-V and GhOST data points during this flight (i.e. also sections not shown in (a,b)). The GLORIA data points are plotted at 75 % transparency to visualise accumulations. The data points of the in situ observations are connected by dashed lines to visualise their temporal sequence (dashed lines do not represent measurement data).

In Fig. 6b, we compare the vertical cross section derived from the GLORIA observations with the HAGAR-V and GhOST observations in a meridional projection. The in situ observations in section A clearly confirm the tropospheric filament detected by GLORIA. Furthermore, low mixing ratios at higher altitudes are confirmed by the in situ observations during sections B and C. Note that even small-scale structures observed by the in situ observations during section C are reproduced to some degree by the GLORIA observations, such as a narrow vertically aligned filamentary structure at ~52°N at the beginning of section C. Also from a quantitative point of view, the GLORIA observations are consistent with the HAGAR-V and GhOST observations. While during sections B and C, low CH_2Cl_2 abundances observed by the instruments agree well in terms of absolute numbers (except of a low-bias of GLORIA during leg C), GLORIA detects typically 20 % to 50 % lower volume mixing ratios than the in situ instruments in the filament during leg A (see Appendix B). These discrepancies can be explained by differences in the sampling (i.e. different sampling geometries and limited vertical and horizontal resolution of GLORIA, see Sect. 2.2 and Woiwode et al. (2018)). In particular, GLORIA observations of a confined local filament can be negative-biased by air masses poor in the same species along the line-of-sight in front and behind the filament.

All CH_2Cl_2 data points available for this flight from GLORIA, HAGAR-V and GhOST above 7 km are shown in Fig. 6c. For GLORIA, also data points after IV, which were omitted in Fig. 6a,b for clarity, are included (compare section after IV in Fig 6a with Fig. 3b). While the GLORIA data points are characterised by noticeably more scattering, they are in general consistent with the in situ data points at all altitudes. At low CH_2Cl_2 abundances, the in situ data points coincide with sections where GLORIA data points scatter densely. Denser populations of GLORIA data points around 100 pptv to 200 pptv between 11 km and 13 km are framed by the in situ data points. Overall, a high degree of consistency of the GLORIA and in situ observations is confirmed by the comparison in Fig. 6 when reminding that remote sensing and in situ observations are compared in a filamentary scenario.

5 Transport pathways and origin of CH_2Cl_2-rich filaments

Transport pathways and possible source regions of CH_2Cl_2-rich filaments observed during research flights F08 on 26 to 27 August 2023 and F17 on 16 to 17 September 2023 are analysed using the CLaMS model. For both flights we apply back-trajectories to analyse transport pathways and identify potential source regions of the observed filaments in the Earth's boundary layer. For the flight on 16 to 17 September 2023 we furthermore apply surface-origin tracers (Vogel et al., 2026) to to quantify their fractions contributing to the measured CH_2Cl_2-rich filament.

5.1 Back-trajectories - tropospheric and stratospheric filaments on 26 to 27 August 2023

A compact tropospheric filament and diffuse filaments in the LMS were observed during PHILEAS research flight F08 (see Fig. 3a,b). For the back-trajectories, initialization locations were chosen such that both the tropospheric filament and the diffuse filament in the LMS after waypoint IV are covered (Fig. 7a).

https://doi.org/10.5194/egusphere-2026-3271
Preprint. Discussion started: 14 August 2026

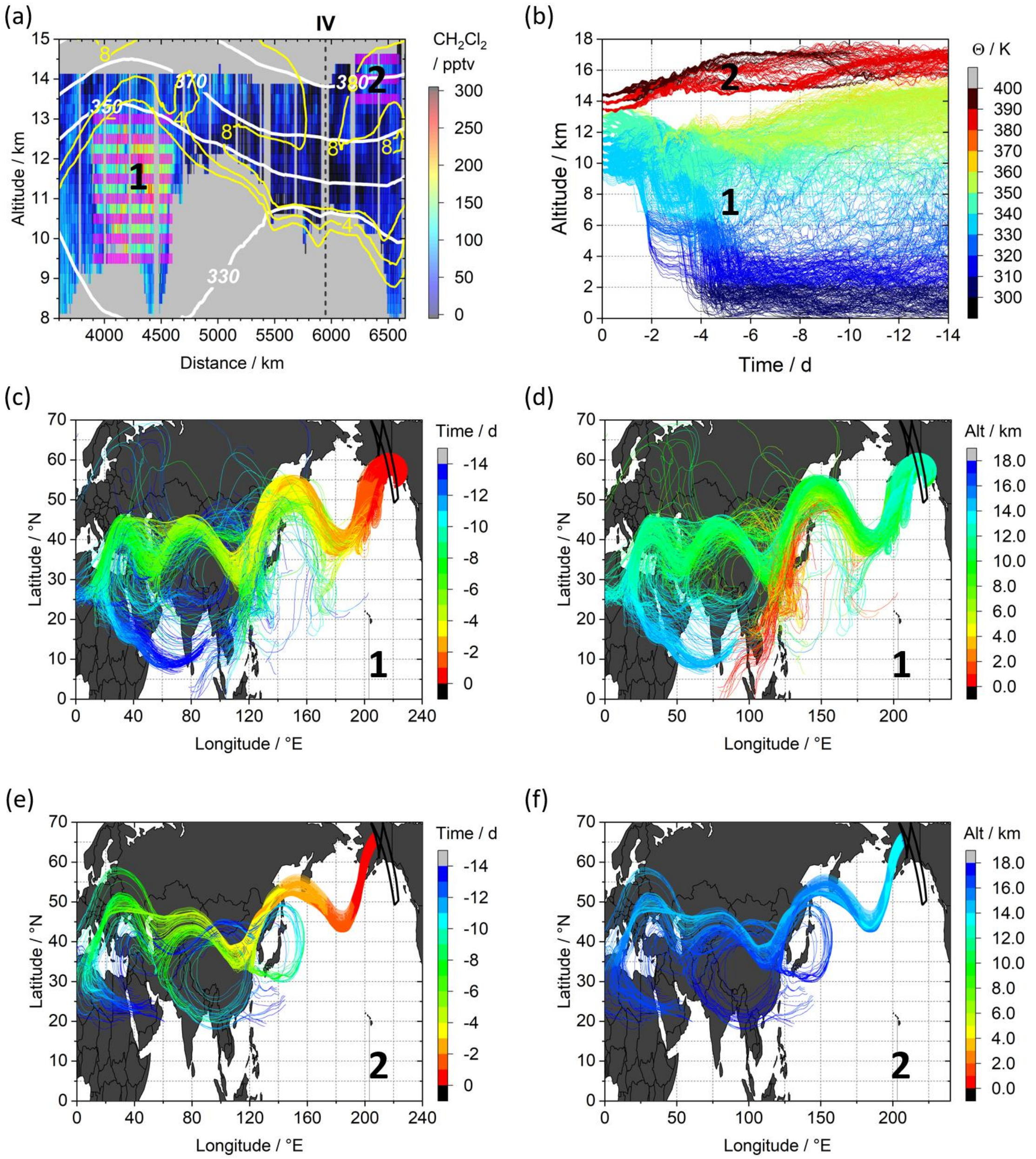

410 **Figure 7.** CLaMS back-trajectories for CH_2Cl_2-rich filaments observed on 26 to 27 August 2023. (a) CH_2Cl_2 volume mixing ratios observed by GLORIA (colour-coded). Starting locations of back-trajectories are superimposed (dense vertical bars in magenta). The tropospheric filament is labelled with "1" and the filament in air masses with LMS character with "2". The corresponding trajectories are differentiated in the subsequent panels. Also shown are potential vorticity isolines (yellow lines) and isentropes (thick white lines) from ECMWF analysis. (b) Vertical motion of trajectories over transport time, colour-coded with isentropic levels (ECMWF ERA5). Yellow to blue trajectories correspond entirely to "1" and red to dark red trajectories entirely to "2". (c,e) Pathways of trajectories with colour-coded transport times in days before the observations and (d,f) pathways of trajectories with colour-coded geopotential height for "1" and "2", respectively.

https://doi.org/10.5194/egusphere-2026-3271
Preprint. Discussion started: 14 August 2026

The tropospheric filament is labelled with “1” and was located below the 4 PVU level and potential temperatures up to 350 K. The filament in the LMS is labelled with “2” and was located slightly below the 8 PVU level (note the folded pattern of the 8 PVU isoline) and potential temperatures around 390 K. The starting locations of the trajectories are indicated schematically by dense magenta vertical bars. For the tropospheric filament (“1”), 736 back-trajectories and for the filament in the LMS (“2”), 164 back-trajectories are analysed over a time interval of 2 weeks.

From the tropospheric filament (“1”), one fraction of the back-trajectories remains in the free troposphere and shows altitude variations within a few kilometres and moderate variations in potential temperature (Fig. 7b). In contrast, another fraction of the trajectories starting from “1” shows strong altitude changes in the magnitude of ~10 km within the time interval from 2 to 6 days before the observations. Many of these trajectories reach the model boundary layer >4 days before the observations. As can be seen in Fig. 7b-d, these altitude changes occurred in the section above the North Pacific and in the vicinity of the northern part of Japan. Further in the past, before reaching the updraft region, these trajectories reside at low altitudes above the coastal region of Eastern China and the South China Sea. This suggests that Eastern China is a likely source region of the CH_2Cl_2-rich filament observed by GLORIA in the troposphere (“1”) above the eastern part of the Gulf of Alaska. Other trajectories associated with “1”, which remain at higher altitudes in the free troposphere, meander further to the west and split above North Africa, with one fraction approaching further from the West and another fraction coming from higher altitudes in the vicinity of the ASM region.

The trajectories starting from the filament in air masses with LMS character (“2”) remain at isentropic levels in the entire time interval of 2 weeks and originate from higher altitudes (Fig. 7b). The main fraction of these back-trajectories meanders to the West towards the Mediterranean region. Above Northeastern China and the Middle East, fractions of trajectories separate, and the resulting fractions form three anticyclonic circulation patterns (Fig 7e,f) centred above the Eastern Mediterranean Region, China and Japan. These regions correspond with the boundary region of the ASMA during the days before the flight (cf. Vogel et al. 2026, their Figs. 13 and C4). Thus, the air masses associated with the filament that was observed by GLORIA in the air masses with LMS character (“2”) originated from higher altitudes at the boundary of the ASMA (cf. Vogel et al., 2026). We mention that further analysis of the same back-trajectories over a longer time interval of 4 weeks (not shown) did not allow to identify a certain source region.

Our results associated with the tropospheric filament (“1”) are consistent with results by Jesswein et al. (2025) who analysed Lagrangian FLEXible PARTicle dispersion model (FLEXPART) trajectories involving ECMWF ERA 5 data for the same flight. Note that their analysis focused on two events at flight level before and during section A, respectively (compare Fig. 6 with Jesswein et al (2025), their Fig. 3), with the second event partly coinciding with the GLORIA observations of the tropospheric filament (“1”). Our results are furthermore consistent with a previous study by Trinkl (2025), who used an earlier version of the CH_2Cl_2 dataset (see also Riese et al., 2025) together with trajectories by the Hybrid Single-Particle Lagrangian Integrated Trajectory Model (HYSPLIT) based on ECMWF ERA 5 data.

https://doi.org/10.5194/egusphere-2026-3271
Preprint. Discussion started: 14 August 2026

5.2 Back-trajectories – tropospheric filament on 16 to 17 September 2023

The highest CH_2Cl_2 abundances during PHILEAS were detected by GLORIA during research flight F17 (Fig. 5a,b). Starting locations of the back-trajectories were chosen such that the strong filament in the southwestern part of the flight is covered (Fig. 8a). The back-trajectories start at tropospheric levels well below 2 PVU and potential temperature levels ≤ 340 K. A total number of 684 back-trajectories is analysed in Figure 8.

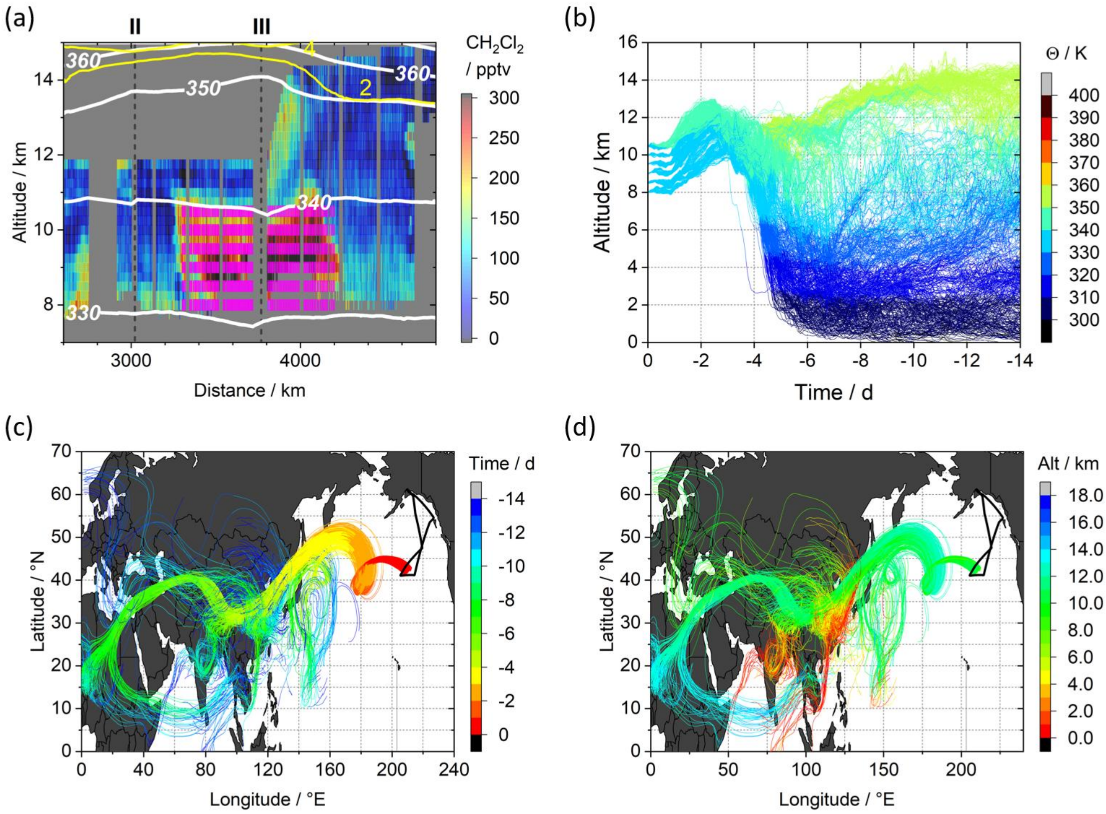

Figure 8. CLaMS back-trajectories for CH_2Cl_2-rich filament observed on 16 to 17 September 2023. For legend, see Fig. 7.

The back-trajectories show moderate altitude variations above the North Pacific and spread into different altitude regimes in the time interval between 3 and 6 days before initialization (Fig. 8b). A fraction of the back-trajectories remains compact at higher altitudes, meanders to the West and partly forms an anticyclonic pattern around the Arabian Sea at altitudes >12 km (Fig. 8c,d). Other fractions of back-trajectories follow a similar path above the North Pacific, but separate whilst approaching the mainland and show strong changes in altitude, partly exceeding 8 km within a period of less than 3 days. Many of these back-trajectories reach the boundary layer above the East China Sea, East China, the Himalayan mountains (where the terrain / model boundary layer is elevated) and North East India. CH_2Cl_2 is known to be primarily emitted from industrialized regions

https://doi.org/10.5194/egusphere-2026-3271
Preprint. Discussion started: 14 August 2026

in Asia (e.g. Feng et al., 2018; Say et al., 2019). Thus, the back-trajectory analysis suggests that East China and India are likely contributors to the CH_2Cl_2-rich filament observed by GLORIA.

Overall, back-trajectory analysis suggests that mainly sources in East China and India contributed to the observed mesoscale filament of CH_2Cl_2-rich air above the Northeastern Pacific. Also in this case, our results are consistent with the results by Jesswein et al. (2025) and Trinkl (2025). When comparing with the results by Jesswein et al. (2025) it should be reminded that in our case a separate filament at lower altitudes is analysed. In the next section, we use surface-origin tracers to gain more insights into possible source regions.

5.3 Surface-origin tracers for observations on 16 to 17 September 2023

To quantify the fractions of different source regions in the Asian monsoon region contributing to the measured CH_2Cl_2-rich filament, surface-origin tracers simulated by CLaMS were interpolated to the times and geolocations of the observations during research flight F17 (Fig. 9). The percentage values of the surface-origin tracers indicate the simulated fraction of air originating since 1 May 2023 from the respective surface region shown in Fig. 9a. If spatial structures with high CH_2Cl_2 volume mixing ratios observed by GLORIA coincide with patterns where a certain surface-origin tracer is enhanced, this suggests that the corresponding surface region is a likely source of the observed emissions.

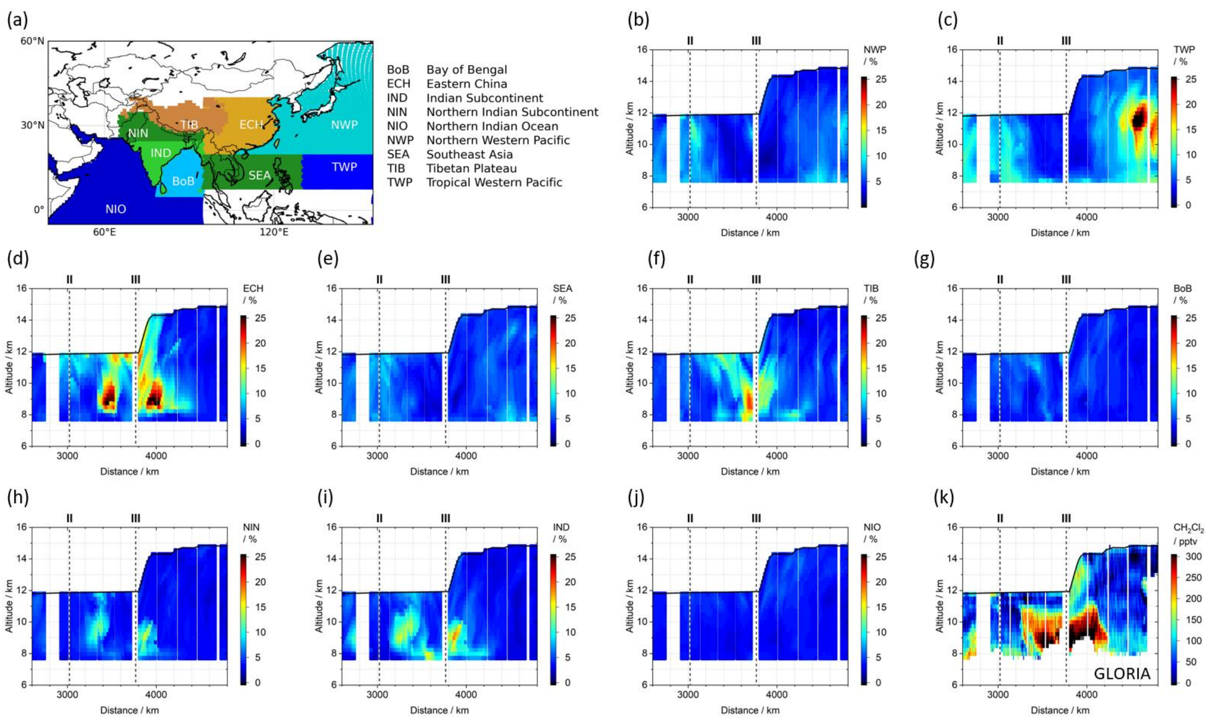

Figure 9. CLaMS surface-origin tracers for the main filament observed during research flight F17 on 16 to 17 September 2023. (a) Release regions of surface-origin tracers in the simulations. (b)-(j) Relative fractions of the respective tracers given in the colourbar title at the geolocations of the observations. (k) CH_2Cl_2 observations by GLORIA.

https://doi.org/10.5194/egusphere-2026-3271
Preprint. Discussion started: 14 August 2026

At the geolocations of the prominent CH_2Cl_2-rich filament in the GLORIA observations (Fig. 9k) coincidences are found with modelled surface-origin tracer fraction maxima associated with Eastern China (ECH, Fig. 9d), the Tibetan Plateau (TIB, Fig. 9f), the North Indian Subcontinent (NIN, Fig. 9h) and the Indian Subcontinent (IND, Fig. 9i). ECH shows the highest surface origin tracer fraction enhancements at similar geolocations as the observed CH_2Cl_2-rich filament, partly exceeding tracer fractions of 25%. Its pattern matches mostly well with the GLORIA observations of CH_2Cl_2-rich air. The spatial distributions of the surface-origin tracers TIB, IND and NIN partly agree with the filament structures observed by GLORIA, but with smaller tracer fractions than simulated for ECH. Thus, CLaMS simulations show that from the simulated source regions, air masses from Eastern China contributed with the highest fraction to the CH_2Cl_2 enhancements observed by GLORIA, followed by regions on the Indian subcontinent and the Himalayas. Both, China as well as India are known anthropogenic source regions of CH_2Cl_2 (e.g. Feng et al., 2018; Say et al., 2019). The Himalayan region is not known as a significant CH_2Cl_2 source due to very little industrial activities (e.g. An et al., 2021). Air masses from this region might possibly contain CH_2Cl_2 due to low-level transport from the Indian Subcontinent. Otherwise, this source region is expected to rather dilute industrial pollution within the observed CH_2Cl_2-rich filament with “clean” mountain air.

6 Discussion and Conclusions

During PHILEAS research flights in August and September 2023, filaments of up to ~1000 km in size and CH_2Cl_2 volume mixing ratios of locally up to ~400 pptv were observed by the airborne limb imager GLORIA above the North Pacific, Canada and Alaska. For the new CH_2Cl_2 retrieval from GLORIA observations, we applied yet unpublished high-resolution CH_2Cl_2 absorption cross sections (Harrison, in preparation), resulting in ~11 % lower volume mixing ratios than previous retrievals (Riese et al., 2025; Trinkl, 2025), where we applied commonly available absorption cross sections of CH_2Cl_2 (Sharpe et al., 2004; Gordon et al., 2022). Consistency of the GLORIA observations with in situ observations by HAGAR-V and GhOST is demonstrated for PHILEAS research flight F08 on 26 and 27 August 2023. While at low CH_2Cl_2 abundances, only small differences are found in terms of absolute volume mixing ratios, GLORIA underestimates the in situ observations by typically 20 % to 50 % at higher CH_2Cl_2 abundances peaking around 250 pptv. The comparison suggests that the CH_2Cl_2 levels inferred from GLORIA observations, which are affected by vertical and horizontal smoothing characteristics of remote sensing observations in limb geometry, represent a conservative estimate of local CH_2Cl_2 abundances.

Highest abundances of CH_2Cl_2 in the GLORIA observations were observed in the free troposphere at potential temperature levels between 320 K and 360 K and resulted from levels below the vertical regime of the ASMA (cf. Ploeger et al., 2015), consistent with Jesswein et al. (2025). Peak levels of CH_2Cl_2 detected by GLORIA are by more than a factor of 6 higher than the northern hemispheric background in that season (cf. AGAGE network, https://www-air.larc.nasa.gov/missions/agage/static/figures/monthly/pdf/ CH2Cl2_mm.pdf; accessed on 25 March 2026). Observed levels exceed previously reported abundances in the ASM region and its western boundary region above Nepal, Northern India and the mediterranean region in 2016 and 2017 (Adcock et al., 2021), above various other regions (Leedham Elvidge et al., 2015,

https://doi.org/10.5194/egusphere-2026-3271
Preprint. Discussion started: 14 August 2026

Lauther et al., 2022), above northern America (Smith et al., 2024), and in the outflow of the 2023 ASM region (Jesswein et al., 2025; Riese et al., 2025; Vogel et al., 2026). Peak CH_2Cl_2 abundances of ~400 pptv detected by GLORIA are lower than maximum values of ~600 pptv reported by Pan et al. (2024) in the upper tropical troposphere in the vicinity of the east ASM region in summer 2022. The GLORIA observations provide a new insight that high CH_2Cl_2 volume mixing ratios can be present locally far downstream of the source regions after transport over long distances across the North Pacific.

CLaMS back-trajectory analysis based on ECMWF ERA5 data to the tropospheric CH_2Cl_2-rich filament observed on 26 to 27 August 2023 confirms that the observed air masses were transported above the North Pacific within only a few days. The back-trajectories also suggest that the main source region of this filament is located at the eastern part of China. This is consistent with the results from Jesswein et al. (2025) and plausible because particularly high CH_2Cl_2 emissions are expected from that region (Oram et al., 2017, An et al., 2021). During PHILEAS, the highest CH_2Cl_2 levels were observed in the troposphere above the North Pacific during the flight on 16 to 17 September 2023. CLaMS back-trajectories and surface-origin tracers (based on ECMWF ERA5 data) suggest that Eastern China and, to a lesser degree, the Indian subcontinent are likely source regions. We mention briefly that elongated diffuse CH_2Cl_2 enhancements against background air were also detected by GLORIA at tropospheric levels and in the tropopause region in the westward outflow of the ASM region above the Mediterranean region early in August 2023 (see example in Appendix C, for flight details, see Riese et al., 2025). As discussed by Vogel et al. (2026), the westward outflow of the ASMA originates mainly from the Indian subcontinent.

During PHILEAS research flight F08, GLORIA detected CH_2Cl_2 levels of up to ~125 pptv locally in air masses with characteristics of the extra-tropical lowermost stratosphere. Back-trajectory analysis suggests that these air masses originated from horizontal isentropic transport of filaments from the boundary region of the ASMA into the extratropical LMS (e.g. Vogel et al., 2016, 2026; Ploeger et al., 2017). In this case, a certain defined source or updraft region is not identified by our analysis because the time scales of air mass transport are longer than those covered by our back-trajectory analysis.

In combination with the CLaMS simulations, the GLORIA observations provide new insights on how large CH_2Cl_2-rich filaments are transported within a few days from the ASM region across the North Pacific, where they can mix with ambient air, and contribute to CH_2Cl_2 abundances in the Northern Hemisphere UTLS. The year-to-year variability of uplift processes in the ASM system, changes in CH_2Cl_2 emissions, and transport efficiency of CH_2Cl_2-rich air masses from the ASM region into the free troposphere and the UTLS remain aspects which should be investigated further. We suggest assessing the potential of deriving CH_2Cl_2 volume mixing ratios from past and possible future satellite-based infrared limb observers. More and continuous observations from ground-based, airborne, and satellite platforms could help to further improve our understanding of how CH_2Cl_2 is transported into the global UTLS region and its role in stratospheric ozone depletion.

https://doi.org/10.5194/egusphere-2026-3271
Preprint. Discussion started: 14 August 2026

Appendix A: Comparison of CH_2Cl_2 absorption cross sections and retrieval results

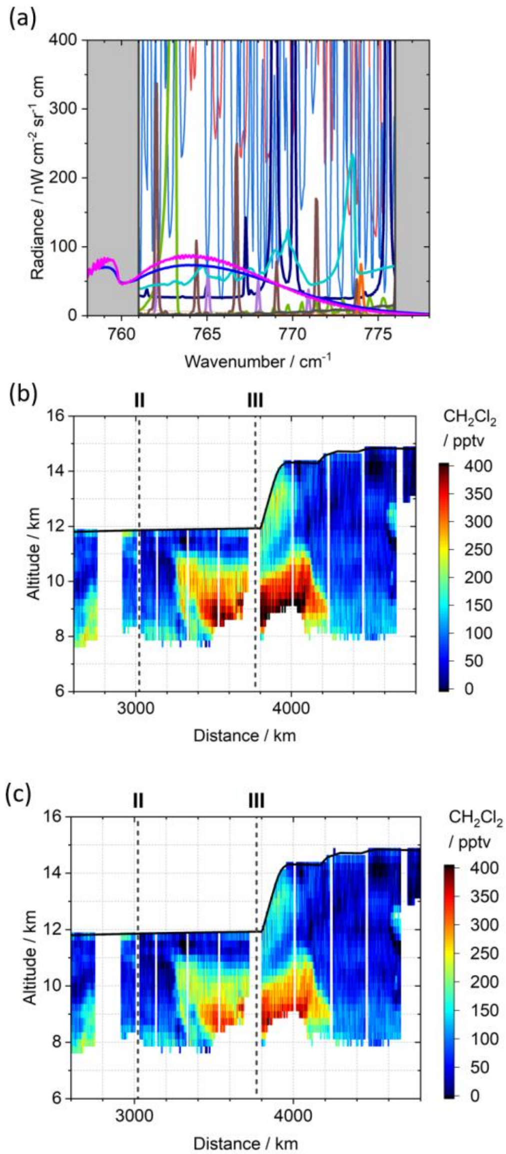

Figure A1. Comparison of spectral signature and retrieval results based on two absorption cross section datasets. (a) Microwindow used for CH_2Cl_2 retrieval (non-shaded region) and spectral signature of CH_2Cl_2 simulated for a tangent altitude of 8 km and CH_2Cl_2 levels of 100 pptv in the troposphere using absorption cross sections available via the HITRAN website (thick blue line; see Sharpe et al. 2004 and Gordon et al., 2022) and the new absorption cross sections by Harrison (in preparation) (magenta). Signatures by interfering gases are shown in red (CO_2), blue (O_3), dark blue (H_2O), cyan (CCl_4), green (HNO_3), brown (C_2H_2), light pink (HCN) and COF_2 (orange). Retrieved volume mixing ratios associated with a subsection of Fig. 5a using (b) absorption cross sections available via the HITRAN website and (c) new absorption cross sections by Harrison (in preparation), which were applied in this study.

https://doi.org/10.5194/egusphere-2026-3271
Preprint. Discussion started: 14 August 2026

Figure A1 shows the same simulation of a limb view as Figure 1b, which involves the new absorption cross sections by Harrison (in preparation). Also shown is the simulated spectral signature of CH_2Cl_2 using the absorption cross sections of Sharpe et al. (2004), which are currently available in HITRAN (Gordon et al., 2022). The simulated radiances in the microwindow used for the GLORIA retrieval, which corresponds with the R-branch region of the υ_9-band of CH_2Cl_2, peak at higher values when using the new absorption cross sections because of the enhanced intensities of these features at lower temperatures. As a consequence, lower maximum values of 400 pptv are obtained (Fig. A1c) when compared to the retrieval using the absorption cross sections of Sharpe et al. (2004) (Fig. A1b). In the latter case, which was applied for the results presented by Riese et al. (2025) and Trinkl (2025), we obtained ~11 % higher peak values of up to ~450 pptv.

Appendix B: In situ comparisons for individual flight legs on 26 to 27 August 2023

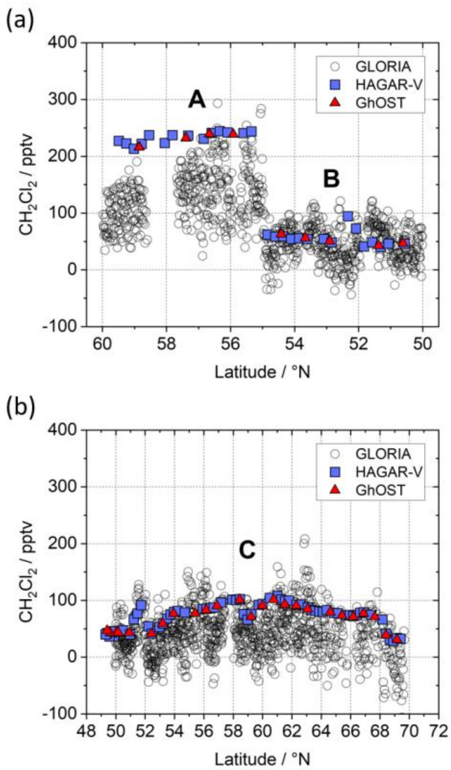

Figure B1. Comparison of GLORIA observations with HAGAR-V and GhOST observations during research flight F08 on 26 and 27 August 2023 at legs A, B and C (compare Fig. 6).

In Figure B1, GLORIA observations at 12.50 km ± 0.25 km (sub-leg A), 13.50 km ± 0.25 km (sub-leg B) and 14.00 km ± 0.25 km (sub-leg C) are compared with HAGAR-V and GhOST observations during PHILEAS research flight F08. The geometries of the comparison are discussed in Sect. 4.

https://doi.org/10.5194/egusphere-2026-3271
Preprint. Discussion started: 14 August 2026

Appendix C: CH_2Cl_2 observations by GLORIA in the western ASM region

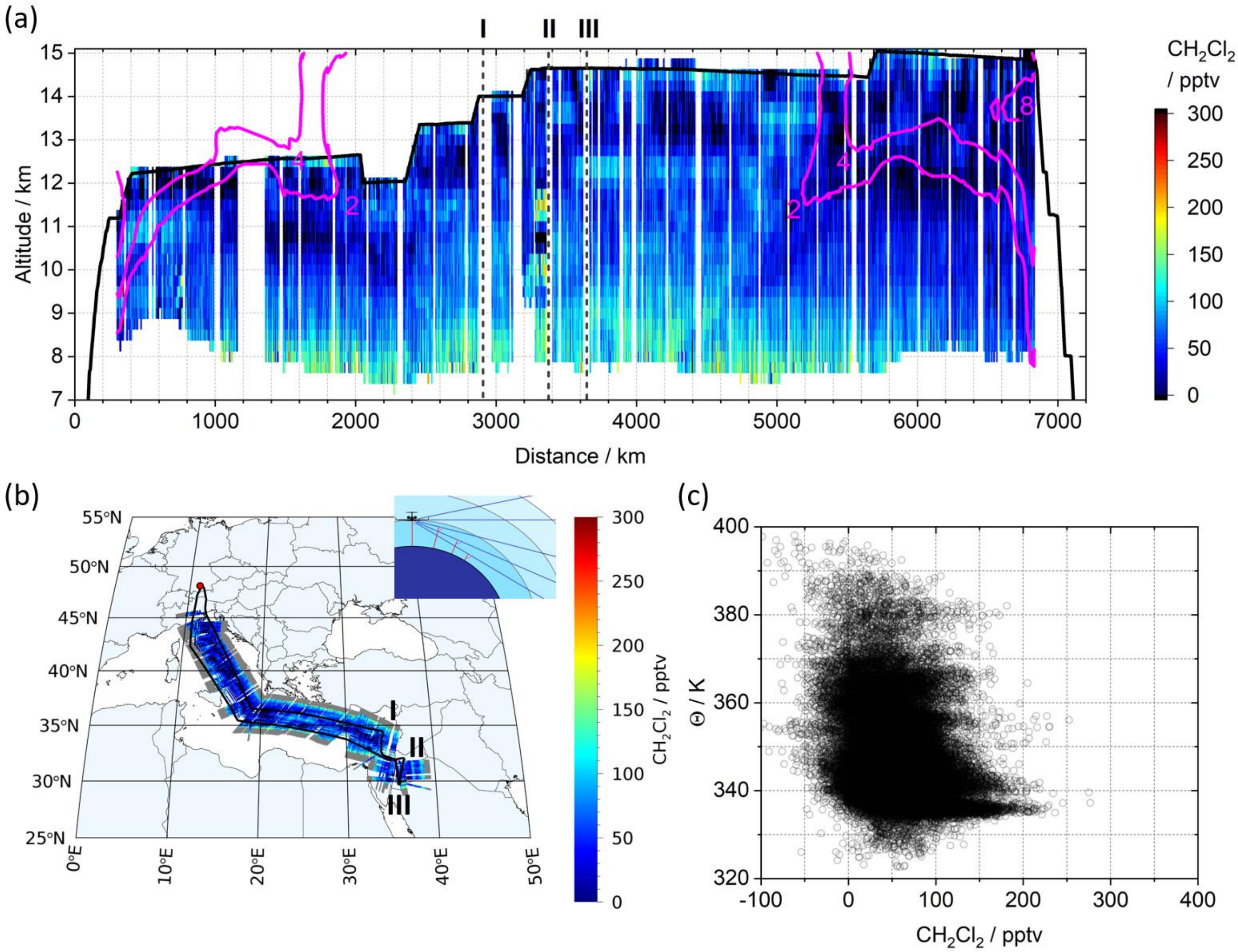

Figure C1. CH_2Cl_2 distribution in the Mediterranean as observed by GLORIA during PHILEAS research flight F02 on 6 August 2023. For plotting details, see Fig. 3.

CH_2Cl_2 observations by GLORIA during PHILEAS research flight F02 are shown in Figure C1. In the eastern part, the observations covered tropospheric air masses in the westward outflow of the ASM (Riese et al., 2025). A tropopause fold was probed during the western parts of the flight. GLORIA observed elongated diffuse structures with moderately enhanced CH_2Cl_2 levels mostly peaking around ~150 pptv at tropospheric altitudes and local CH_2Cl_2 enhancements also in the tropopause fold. Note that the pattern between altitudes of 9 km and 12 km shortly before reaching waypoint II is overemphasised due to oscillations in the retrieval in the presence of thin clouds.

https://doi.org/10.5194/egusphere-2026-3271
Preprint. Discussion started: 14 August 2026

Author contributions

Instrument operations, flight monitoring, data processing and data evaluation during and after PHILEAS were done for GLORIA by MD, FFV, NG, TG, MH, SJ, JK, AK, EK, GM, TN, HN, CP, PP, MRe, MR, SR, HR, GS, FT, JU, GW, and WW, for HAGAR-V by VL, JS, RVL, and CMV, and for GhOST by AE, MJ, TK, and TS. BV, JUG, and FP performed the CLaMS simulations and trajectory calculations used here and for flight planning. JH provided the new absorption cross sections of CH_2Cl_2. Study concept and manuscript were elaborated by WW together with VL, BV, JUG, and involving suggestions by the other coauthors. The CH_2Cl_2 retrieval was elaborated by WW and implemented with the help of SJ and NG. Planning of the flights that are in focus here was led by PH, FP, and MR together with the PHILEAS flight planning team. SV provided ICON-ART simulations, which were helpful for GLORIA flight planning. PHILEAS was coordinated by MR and PH together with the PHILEAS coordination team. All authors helped shaping the manuscript.

Acknowledgements

We acknowledge support by the German Research Foundation for funding parts of the PHILEAS mission within the HALO SPP 1294. We thank the Helmholtz society and the Helmholtz centres KIT and JÜLICH for supporting atmospheric research with HALO within the PoF research field Earth and Environment. We thank DLR-FX for performing the HALO operations flexibly and reliably. We thank the ECMWF for providing the meteorological data.

Financial support

This research has been supported by the German Research Foundation (Deutsche Forschungsgemeinschaft, DFG Priority Program SPP 1294, DFG Project number 316646266 and contributes to the projects no. VO 1276/7-1 and HO 4120/4-1. This study also contributed to the ESA CAIRTEX project no. 4000141036/23/NL/FF/ab.

Conflicts of interests

At least one of the (co-)authors is a member of the editorial board of Atmospheric Chemistry and Physics. The authors have no other competing interests to declare.

Data availability

The GLORIA data are publicly available at RADAR4KIT via https://radar.kit.edu/radar/en/dataset/5xbxp3huqgq814ea (Johansson, 2026). The HAGAR-V, GhOST data are accessible at the HALO database via https://doi.org/10.17616/R39Q0T (HALO, 2026). Results of the CLaMS simulations presented in this work are available from Bärbel Vogel upon request.

https://doi.org/10.5194/egusphere-2026-3271
Preprint. Discussion started: 14 August 2026

ECMWF ERA5 data are accessible via https://www.ecmwf.int/en/forecasts/dataset/ecmwf-reanalysis-v5 (Hersbach et al., 2023).

References

Adcock, K. E., Fraser, P. J., Hall, B. D., Langenfelds, R. L., Lee, G., Montzka, S. A., Oram, D. E., Röckmann, T., Stroh, F., Sturges, W. T., Vogel, B., and Laube, J. C.: Aircraft-Based Observations of Ozone-Depleting Substances in the Upper Troposphere and Lower Stratosphere in and Above the Asian Summer Monsoon, J. Geophys. Res.-Atmos., 126, e2020JD033137, https://doi.org/10.1029/2020JD033137, 2021.

An, M., Western, L. M., Say, D., Chen, L., Claxton, T., Ganesan, A. L., Hossaini, R., Krummel, P. B., Manning, A. J., Mühle, J., O'Doherty, S., Prinn, R. G., Weiss, R. F., Young, D., Hu, J., Yao, B., and Rigby, M.: Rapid increase in dichloromethane emissions from China inferred through atmospheric observations, Nature Communications, 12, https://doi.org/10.1038/s41467-021-27592-y, 2021.

Bauchinger, S., Engel, A., Jesswein, M., Keber, T., Bönisch, H., Obersteiner, F., Zahn, A., Emig, N., Hoor, P., Lachnitt, H.-C., Weyland, F., Ort, L., and Schuck, T. J.: The extratropical tropopause – trace gas perspective on tropopause definition choice, Atmos. Chem. Phys., 25, 14167–14186, https://doi.org/10.5194/acp-25-14167-2025, 2025.

Chipperfield, M. P., Hossaini, R., Montzka, S. A., Reimann, S., Sherry, D., and Tegtmeier, S.: Renewed and emerging concerns over the production and emission of ozone-depleting substances. Nature Reviews Earth & Environment, 1(5), 251–263. https://doi.org/10.1038/s43017-020-0048-8, 2020.

Claxton, T., Hossaini, R., Wild, O., Chipperfield, M. P., and Wilson, C.: On the regional and seasonal ozone depletion potential of chlorinated very short-lived substances, Geophys. Res. Lett., 46, 5489–5498, https://doi.org/10.1029/2018GL081455, 2019.

Claxton, T., Hossaini, R., Wilson, C., Montzka, S. A., Chipperfield, M. P., Wild, O., Bednarz, E. M., Carpenter, L. J., Andrews, S. J., Hackenberg, S. C., Mühle, J., Oram, D., Park, S., Park, M., Atlas, E., Navarro, M., Schauffler, S., Sherry, D., Vollmer, M., Schuck, T., Engel, A., Krummel, P. B., Maione, M., Arduini, J., Saito, T., Yokouchi, Y., O'Doherty, S., Young, D., and Lunder, C.: A synthesis inversion to constrain global emissions of two very short lived chlorocarbons: dichloromethane, and perchloroethylene, J. Geophys. Res.-Atmos., 125, e2019JD031818, https://doi.org/10.1029/2019JD031818, 2020.

Clemens, J., Ploeger, F., Konopka, P., Portmann, R., Sprenger, M., and Wernli, H.: Characterization of transport from the Asian summer monsoon anticyclone into the UTLS via shedding of low potential vorticity cutoffs, Atmos. Chem. Phys., 22, 3841–3860, https://doi.org/10.5194/acp-22-3841-2022, 2022.

Dubé, K., Tegtmeier, S., Bourassa, A., Laube, J. C., Engel, A., Saunders, L. N., Walker, K. A., Hossaini, R., and Bednarz, E. M.: Chlorinated very short-lived substances offset the long-term reduction of inorganic stratospheric chlorine. Commun Earth Environ. 6, 487, https://doi.org/10.1038/s43247-025-02478-9, 2025.

https://doi.org/10.5194/egusphere-2026-3271
Preprint. Discussion started: 14 August 2026

Dunkerton, T. J.: Evidence of meridional motion in the summer lower stratosphere adjacent to monsoon regions, J. Geophys. Res.-Atmos., 100, 16675–16688, https://doi.org/10.1029/95JD01263, 1995

Engel, A., Rigby, M., Burkholder, J. B., Fernandez, R. P., Froidevaux, L., Hall, B. D., Hossaini, R., Saito, T., Vollmer, M. K., and Yao, B.: Update on ozone-depleting substances (ODSs) and other gases of interest to the Montreal protocol, Chapter 1, in: Scientific Assessment of Ozone Depletion: 2018, Global Ozone Research and Monitoring Project – Report No. 58, WMO, 1–87, ISBN 978-1-7329317-1-8, 2018.

Feng, Y., Bie, P., Wang, Z., Wang, L., and Zhang, J.: Bottom-up anthropogenic dichloromethane emission estimates from China for the period 2005–2016 and predictions of future emissions, Atmos. Environ., 186, 241–247, https://doi.org/10.1016/j.atmosenv.2018.05.039, 2018.

Friedl-Vallon, F., Gulde, T., Hase, F., Kleinert, A., Kulessa, T., Maucher, G., Neubert, T., Olschewski, F., Piesch, C., Preusse, P., Rongen, H., Sartorius, C., Schneider, H., Schönfeld, A., Tan, V., Bayer, N., Blank, J., Dapp, R., Ebersoldt, A., Fischer, H., Graf, F., Guggenmoser, T., Höpfner, M., Kaufmann, M., Kretschmer, E., Latzko, T., Nordmeyer, H., Oelhaf, H., Orphal, J., Riese, M., Schardt, G., Schillings, J., Sha, M. K., Suminska-Ebersoldt, O., and Ungermann, J.: Instrument concept of the imaging Fourier transform spectrometer GLORIA, Atmos. Meas. Tech., 7, 3565–3577, https://doi.org/10.5194/amt-7-3565-2014, 2014.

Ganeff, J.M. and Jungers, J.C.: Tensions de Vapeur du Systeme CH_3Cl - CH_2Cl_2, Bull. Soc. Chim. Belg., 57, 1-3, 82-87, https://doi.org/10.1002/bscb.19480570109, 1948.

Geldenhuys, M., Kaifler, B., Preusse, P., Ungermann, J., Alexander, P., Krasauskas, L., Rhode, S., Woiwode, W., Ern, M., Rapp, M., and Riese, M.: Observations of gravity wave refraction and its causes and consequences. Journal of Geophysical Research: Atmospheres, 128(3), e2022JD036830. https://doi.org/10.1029/2022JD036830, 2023.

Gordon, I.E., Rothman, L.S., Hargreaves, R.J., Hashemi, R., Karlovets, E.V., Skinner, F.M., Conway, E.K., Hill, C., Kochanov, R.V., Tan, Y., Wcisło, P., Finenko, A.A., Nelson, K., Bernath, P.F., Birk, M., Boudon, V., Campargue, A., Chance, K.V., Coustenis, A.,. Drouin, B.J, Flaud, J.–M., Gamache, R.R., Hodges, J.T., Jacquemart, D., Mlawer, E.J., Nikitin, A.V., Perevalov, V.I., Rotger, M., Tennyson, J., Toon, G.C., Tran, H., Tyuterev, V.G., Adkins, E.M., Baker, A., Barbe, A., Canè, E., Császár, A.G., Dudaryonok, A., Egorov, O., Fleisher, A.J., Fleurbaey, H., Foltynowicz, A., Furtenbacher, T., Harrison, J.J., Hartmann, J.–M., Horneman, V.–M., Huang, X., Karman, T., Karns, J., Kassi, S., Kleiner, I., Kofman, V., Kwabia–Tchana, F., Lavrentieva, N.N., Lee, T.J., Long, D.A., Lukashevskaya, A.A., Lyulin, O.M., Makhnev, V.Yu., Matt, W., Massie, S.T., Melosso, M., Mikhailenko, S.N., Mondelain, D., Müller, H.S.P., Naumenko, O.V., Perrin, A., Polyansky, O.L., Raddaoui, E., Raston, P.L., Reed, Z.D., Rey, M., Richard, C., Tóbiás, R., Sadiek, I., Schwenke, D.W., Starikova, E., Sung, K., Tamassia, F., Tashkun, S.A., Vander Auwera, J., Vasilenko, I.A., Vigasin, A.A., Villanueva, G.L., Vispoel, B., Wagner, G., Yachmenev, A., and Yurchenko, S.N.: The HITRAN2020 molecular spectroscopic database, Journal of Quantitative Spectroscopy and Radiative Transfer, 277, 107949, https://doi.org/10.1016/j.jqsrt.2021.107949, 2022.

HALO: HALO database, re3data.org - Registry of Research Data Repositories, https://doi.org/10.17616/R39Q0T, editing status 2025-11-25, last accessed: 2026-04-10, 2026.

Harrison, J.J., in preparation.

Hersbach, H., Bell, B., Berrisford, P., Hirahara, S., Horányi, A., Muñoz-Sabater, J., Nicolas, J., Peubey, C., Radu, R., Schepers, D., Simmons, A., Soci, C., Abdalla, S., Abellan, X., Balsamo, G., Bechtold, P., Biavati, G., Bidlot, J., Bonavita, M., De Chiara, G., Dahlgren, P., Dee, D., Diamantakis, M., Dragani, R., Flemming, J., Forbes, R., Fuentes, M., Geer, A., Haimberger, L., Healy, S., Hogan, R. J., Hólm, E., Janisková, M., Keeley, S., Laloyaux, P., Lopez, P., Lupu, C., Radnoti, G., de Rosnay, P., Rozum, I., Vamborg, F., Villaume, S., and Thépaut, J.-N.: The ERA5 global reanalysis, Q. J. Roy. Meteorol. Soc., 146, 1999–2049, https://doi.org/10.1002/qj.3803, 2020.

Hersbach, H., Bell, B., Berrisford, P., Biavati, G., Horányi, A., Muñoz Sabater, J., Nicolas, J., Peubey, C., Radu, R., Rozum, I., Schepers, D., Simmons, A., Soci, C., Dee, D., Thépaut, J-N.: ERA5 hourly data on pressure levels from 1940 to present. Copernicus Climate Change Service (C3S) Climate Data Store (CDS), DOI: 10.24381/cds.bd0915c6, 2023.

Höpfner, M., Blom, C. E., Echle, G., Glatthor, N., Hase, F., and Stiller, G.: Retrieval simulations for MIPAS-STR measurements, in: Proc. of the Int. Radiation Symp., edited by: Smith, W. L., St. Petersburg, Russia, 24–29 July 2000, DEEPAK Publ., Hampton, Va., 2001.

Höpfner, M., Ungermann, J., Borrmann, S., Wagner, R., Spang, R., Riese, M., Stiller, G., Appel, O., Batenburg, A. M., Bucci, S., Cairo, F., Dragoneas, A., Friedl-Vallon, F., Hünig, A., Johansson, S., Krasauskas, L., Legras, B., Leisner, T., Mahnke, C., Möhler, O., Molleker, S., Müller, R., Neubert, T., Orphal, J., Preusse, P., Rex, M., Saathoff, H., Stroh, F., Weigel, R., and Wohltmann, I.: Ammonium nitrate particles formed in upper troposphere from ground ammonia sources during Asian monsoons, Nat. Geosci., 12, 608–612, https://doi.org/10.1038/s41561-019-0385-8, 2019.

Holton, J. R., Haynes, P. H., McIntyre, M. E., Douglass, A. R., Rood, R. B., and Pfister, L.: Stratosphere-Troposphere Exchange, Rev. Geophys., 33, 403–439, https://doi.org/10.1029/95rg02097, 1995.

Hossaini, R., Chipperfield, M. P., Saiz-Lopez, A., Harrison, J. J., von Glasow, R., Sommariva, R., Atlas, E., Navarro, M., Montzka, S. A., Feng, W., Dhomse, S., Harth, C., Mühle, J., Lunder, C., O'Doherty, S., Young, D., Reimann, S., Vollmer, M. K., Krummel, P. B., and Bernath, P. F.: Growth in stratospheric chlorine from short-lived chemicals not controlled by the Montreal Protocol, Geophys. Res. Lett., 42, 4573–4580, https://doi.org/10.1002/2015gl063783, 2015.

Hossaini, R., Chipperfield, M. P., Montzka, S. A., Leeson, A. A., Dhomse, S. S., and Pyle, J. A.: The increasing threat to stratospheric ozone from dichloromethane, Nat. Commun., 8, 15962, https://doi.org/10.1038/ncomms15962, 2017.

Jesswein, M., Bozem, H., Lachnitt, H.-C., Hoor, P., Wagenhäuser, T., Keber, T., Schuck, T., and Engel, A.: Comparison of inorganic chlorine in the Antarctic and Arctic lowermost stratosphere by separate late winter aircraft measurements, Atmospheric Chemistry and Physics, 21, 17 225–17 241, https://doi.org/10.5194/acp-21-17225-2021, 2021.

Jesswein, M., Lauther, V., Emig, N., Hoor, P., Keber, T., Lachnitt, H.-C., Ort, L., Schuck, T., Strobel, J., Van Luijt, R., Volk, C. M., Weyland, F., and Engel, A.: Tracing elevated abundance of CH_2Cl_2 in the subarctic upper troposphere to the Asian Summer Monsoon, Atmos. Chem. Phys., 25, 8107–8126, https://doi.org/10.5194/acp-25-8107-2025, 2025.

Johansson, Sören: GLORIA PHILEAS Level2 (Version 2026-03-17). Johansson, Sören; Höpfner, Michael. DOI: 10.35097/5xbxp3huqgq814ea (last access: April 2026), 2026.

Johansson, S., Woiwode, W., Höpfner, M., Friedl-Vallon, F., Kleinert, A., Kretschmer, E., Latzko, T., Orphal, J., Preusse, P., Ungermann, J., Santee, M. L., Jurkat-Witschas, T., Marsing, A., Voigt, C., Giez, A., Krämer, M., Rolf, C., Zahn, A., Engel, A., Sinnhuber, B.-M., and Oelhaf, H.: Airborne limb-imaging measurements of temperature, HNO_3, O_3, $ClONO_2$, H_2O and CFC-12 during the Arctic winter 2015/2016: characterization, in situ validation and comparison to Aura/MLS, Atmos. Meas. Tech., 11, 4737–4756, https://doi.org/10.5194/amt-11-4737-2018, 2018.

Johansson, S., Wetzel, G., Friedl-Vallon, F., Glatthor, N., Höpfner, M., Kleinert, A., Neubert, T., Sinnhuber, B.-M., and Ungermann, J.: Biomass burning pollution in the South Atlantic upper troposphere: GLORIA trace gas observations and evaluation of the CAMS model, Atmos. Chem. Phys., 22, 3675–3691, https://doi.org/10.5194/acp-22-3675-2022, 2022.

Keber, T., Bönisch, H., Hartick, C., Hauck, M., Lefrancois, F., Obersteiner, F., Ringsdorf, A., Schohl, N., Schuck, T., Hossaini, R., Graf, P., Jöckel, P., and Engel, A.: Bromine from short-lived source gases in the extratropical northern hemispheric upper troposphere and lower stratosphere (UTLS), Atmospheric Chemistry and Physics, 20, 4105–4132, https://doi.org/10.5194/acp-20-4105-2020, 2020.

Krasauskas, L., Ungermann, J., Preusse, P., Friedl-Vallon, F., Zahn, A., Ziereis, H., Rolf, C., Plöger, F., Konopka, P., Vogel, B., and Riese, M.: 3-D tomographic observations of Rossby wave breaking over the North Atlantic during the WISE aircraft campaign in 2017, Atmos. Chem. Phys., 21, 10249–10272, https://doi.org/10.5194/acp-21-10249-2021, 2021.

Laube, J. C., Schuck, T. J., Baartman, S., Chen, H., Geldenhuys, M., van Heuven, S., Keber, T., Popa, M. E., Tuffnell, E., Voet, F., Vogel, B., Wagenhäuser, T., Zanchetta, A., and Engel, A.: Vertical distribution of halogenated trace gases in the summer Arctic stratosphere based on two independent air sampling methods, Atmos. Meas. Tech., 18, 4087–4102, https://doi.org/10.5194/amt-18-4087-2025, 2025.

Lauther, V., Vogel, B., Wintel, J., Rau, A., Hoor, P., Bense, V., Müller, R., and Volk, C. M.: In situ observations of CH_2Cl_2 and $CHCl_3$ show efficient transport pathways for very short-lived species into the lower stratosphere via the Asian and the North American summer monsoon, Atmos. Chem. Phys., 22, 2049–2077, https://doi.org/10.5194/acp-22-2049-2022, 2022.

Leedham Elvidge, E. C., Oram, D. E., Laube, J. C., Baker, A. K., Montzka, S. A., Humphrey, S., O'Sullivan, D. A., and Brenninkmeijer, C. A. M.: Increasing concentrations of dichloromethane, CH2Cl2, inferred from CARIBIC air samples collected 1998–2012, Atmos. Chem. Phys., 15, 1939–1958, https://doi.org/10.5194/acp-15-1939-2015, 2015.

Li, Q., Jiang, J. H., Wu, D. L., Read, W. G., Livesey, N. J., Waters, J. W., Zhang, Y., Wang, B., Filipiak, M. J., Davis, C. P., Turquety, S., Wu, S., Park, R. J., Yantosca, R. M., and Jacob, D. J.: Convective outflow of South Asian pollution: A global

https://doi.org/10.5194/egusphere-2026-3271
Preprint. Discussion started: 14 August 2026

CTM simulation compared with EOS MLS observations, Geophys. Res. Lett., 32, L14826, https://doi.org/10.1029/2005GL022762, 2005.

Mason, R. B. and Anderson, C. E.: The development and decay of the 100-mb. summertime anticyclone over southern Asia, Mon. Weather Rev., 91, 3–12, https://doi.org/10.1175/1520-0493(1963)091<0003:TDADOT>2.3.CO;2, 1963.

McKenna, D. S.: A new Chemical Lagrangian Model of the Stratosphere (CLaMS) 1. Formulation of advection and mixing, J. Geophys. Res., 107, 1435, https://doi.org/10.1029/2000JD000114, 2002a.

McKenna, D. S.: A new Chemical Lagrangian Model of the Stratosphere (CLaMS) 2. Formulation of chemistry scheme and initialization, J. Geophys. Res., 107, 4256, https://doi.org/10.1029/2000JD000113, 2002b.

Oram, D. E., Ashfold, M. J., Laube, J. C., Gooch, L. J., Humphrey, S., Sturges, W. T., Leedham-Elvidge, E., Forster, G. L., Harris, N. R. P., Mead, M. I., Samah, A. A., Phang, S. M., Ou-Yang, C.-F., Lin, N.-H., Wang, J.-L., Baker, A. K., Brenninkmeijer, C. A. M., and Sherry, D.: A growing threat to the ozone layer from short-lived anthropogenic chlorocarbons, Atmos. Chem. Phys., 17, 11929–11941, https://doi.org/10.5194/acp-17-11929-2017, 2017.

Pan, L. L., Atlas, E. L., Honomichl, S. B., Smith, W. P., Kinnison, D. E., Solomon, S., Santee, M. L., Saiz-Lopez, A., Laube, J. C., Wang, B., Ueyama, R., Bresch, J. F., Hornbrook, R. S., Apel, E. C., Hills, A. J., Treadaway, V., Smith, K., Schauffler, S., Donnelly, S., Hendershot, R., Lueb, R., Campos, T., Viciani, S., D'Amato, F., Bianchini, G., Barucci, M., Podolske, J. R., Iraci, L. T., Gurganus, C., Bui, P., Dean-Day, J. M., Millán, L., Ryoo, J.-M., Barletta, B., Koo, J.-H., Kim, J., Liang, Q., Randel, W. J., Thornberry, T., and Newman, P. A.: East Asian summer monsoon delivers large abundances of very short-lived organic chlorine substances to the lower stratosphere, Proceedings of the National Academy of Sciences, 121, e2318716 121, https://doi.org/10.1073/pnas.2318716121, 2024.

Park, M., Randel, W. J., Gettleman, A., Massie, S. T., and Jiang, J. H.: Transport above the Asian summer monsoon anticyclone inferred from Aura Microwave Limb Sounder tracers, J. Geophys. Res., 112, D16309, https://doi.org/10.1029/2006JD008294, 2007.

Ploeger, F., Gottschling, C., Griessbach, S., Grooß, J.-U., Guenther, G., Konopka, P., Müller, R., Riese, M., Stroh, F., Tao, M., Ungermann, J., Vogel, B., and von Hobe, M.: A potential vorticity-based determination of the transport barrier in the Asian summer monsoon anticyclone, Atmos. Chem. Phys., 15, 13145–13159, https://doi.org/10.5194/acp-15-13145-2015, 2015.

Ploeger, F., Konopka, P., Walker, K., and Riese, M.: Quantifying pollution transport from the Asian monsoon anticyclone into the lower stratosphere, Atmos. Chem. Phys., 17, 7055–7066, https://doi.org/10.5194/acp-17-7055-2017, 2017.

Ploeger, F., Diallo, M., Charlesworth, E., Konopka, P., Legras, B., Laube, J. C., Grooß, J.-U., Günther, G., Engel, A., and Riese, M.: The stratospheric Brewer–Dobson circulation inferred from age of air in the ERA5 reanalysis, Atmos. Chem. Phys., 21, 8393–8412, https://doi.org/10.5194/acp-21-8393-2021, 2021.

Pommrich, R., Müller, R., Grooß, J.-U., Konopka, P., Ploeger, F., Vogel, B., Tao, M., Hoppe, C. M., Günther, G., Spelten, N., Hoffmann, L., Pumphrey, H.-C., Viciani, S., D'Amato, F., Volk, C. M., Hoor, P., Schlager, H., and Riese, M.: Tropical

https://doi.org/10.5194/egusphere-2026-3271
Preprint. Discussion started: 14 August 2026

troposphere to stratosphere transport of carbon monoxide and long-lived trace species in the Chemical Lagrangian Model of the Stratosphere (CLaMS), Geosci. Model Dev., 7, 2895–2916, https://doi.org/10.5194/gmd-7-2895-2014, 2014.

Prinn, R. G., Weiss, R. F., Arduini, J., Arnold, T., DeWitt, H. L., Fraser, P. J., Ganesan, A. L., Gasore, J., Harth, C. M., Hermansen, O., Kim, J., Krummel, P. B., Li, S., Loh, Z. M., Lunder, C. R., Maione, M., Manning, A. J., Miller, B. R., Mitrevski, B., Mühle, J., O'Doherty, S., Park, S., Reimann, S., Rigby, M., Saito, T., Salameh, P. K., Schmidt, R., Simmonds, P. G., Steele, L. P., Vollmer, M. K., Wang, R. H., Yao, B., Yokouchi, Y., Young, D., and Zhou, L.: History of chemically and radiatively important atmospheric gases from the Advanced Global Atmospheric Gases Experiment (AGAGE), Earth Syst. Sci. Data, 10, 985–1018, https://doi.org/10.5194/essd-10-985-2018, 2018.

Riese, M., Oelhaf, H., Preusse, P., Blank, J., Ern, M., Friedl-Vallon, F., Fischer, H., Guggenmoser, T., Höpfner, M., Hoor, P., Kaufmann, M., Orphal, J., Plöger, F., Spang, R., Suminska-Ebersoldt, O., Ungermann, J., Vogel, B., and Woiwode, W.: Gimballed Limb Observer for Radiance Imaging of the Atmosphere (GLORIA) scientific objectives, Atmos. Meas. Tech., 7, 1915–1928, https://doi.org/10.5194/amt-7-1915-2014, 2014.

Riese, M., Hoor, P., Kunkel, D., Vogel, B., Kachula, O., Ploeger, F., Clemens, J., Geldenhuys, M., Guenther, G., Borrmann, S., Engel, A., Fadnavis, S., Friedl-Vallon, F., Grooß, J. U., Hegglin, M. I., Hoepfner, M., Jesswein, M., Johansson, S., Kaumanns, J., Koellner, F., Lauther, V., Mueller, R., Poehlker, M., Rapp, M., Rhode, S., Schneider, J., Schuck, T., Sinnhuber B. M. Tomsche, L., von Hobe, M., Ungermann, J., Versick, S., Voigt, C., Volk, M., Zahn, A., and Ziereis, H.: Long-range transport of polluted Asian summer monsoon air to high latitudes during the PHILEAS campaign in the boreal summer 2023, BAMS, EOR, https://doi.org/10.1175/BAMS-D-24-0232.1, 2025.

Saiz-Lopez, A., Mahajan, A. S., Abbatt, J., Bobrowski, N., Brown, S. S., Burrows, J. P., Carpenter, L. J., Chipperfield, M. P., Cuevas, C. A., Fernandez, R. P., Hossaini, R., Kinnison, D. E., Lamarque, J.-F., Finlayson-Pitts, B. J., Plane, J. M. C., Platt, U., Pratt, K. A., Ravishankara, A. R., Salawitch, R. J., Saltzman, E. S., Simpson, W. R., Solomon, S., Thornton, J. A., and Wang, T.: The influence of short-lived halogens on atmospheric chemistry and climate. Nature 648, 289–299, https://doi.org/10.1038/s41586-025-09753-x, 2025.

Santee, M. L., Manney, G. L., Livesey, N. J., Schwartz, M. J., Neu, J. L., and Read, W. G.: A comprehensive overview of the climatological composition of the Asian summer monsoon anticyclone based on 10 years of Aura Microwave Limb Sounder measurements, J. Geophys. Res., 122, 5491–5514, https://doi.org/10.1002/2016JD026408, 2017.

Say, D., Ganesan, A. L., Lunt, M. F., Rigby, M., O'Doherty, S., Harth, C., Manning, A. J., Krummel, P. B., and Bauguitte, S.: Emissions of halocarbons from India inferred through atmospheric measurements, Atmos. Chem. Phys., 19, 9865–9885, https://doi.org/10.5194/acp-19-9865-2019, 2019.

Schröter, J., Rieger, D., Stassen, C., Vogel, H., Weimer, M., Werchner, S., Förstner, J., Prill, F., Reinert, D., Zängl, G., Giorgetta, M., Ruhnke, R., Vogel, B., and Braesicke, P.: ICON-ART 2.1: a flexible tracer framework and its application for composition studies in numerical weather forecasting and climate simulations, Geosci. Model Dev., 11, 4043–4068, https://doi.org/10.5194/gmd-11-4043-2018, 2018.

Sharpe, S.W., Johnson, T.J., Sams, R.L., Chu, P.M., Rhoderick, G.C., and Johnson, P.A.: Gas-phase databases for quantitative infrared spectroscopy, Appl Spectrosc, 58, 1452-1461, 2004.

Shimanouchi, T., and Suzuki, I.: Infrared spectra and force constants of CH2Cl2, CHDCl2, and CD2Cl2, Journal of Molecular Spectroscopy, Volume 8, Issues 1–6, 222-235, https://doi.org/10.1016/0022-2852(62)90023-1, 1962.

Smith, K., Atlas, E., Apel, E. C., Blake, D. R., Dutton, G., Hornbrook, R. S., Montzka, S., Mühle, J., Schauffler, S., and Treadaway, V.: Chloromethanes in the North American troposphere and lower stratosphere over the past two decades, Geophysical Research Letters, 51, e2024GL108710. https://doi.org/10.1029/2024GL108710, 2024.

Spang, R., Remedios, J. J., and Barkley, M. P.: Colour indices for the detection and differentiation of cloud types in infra-red limb emission spectra, Adv. Space Res., 33, 1041–1047, 2004.

Stiller, G. P., von Clarmann, T., Funke, B., Glatthor, N., Hase, F., Höpfner, M., and Linden, A.: Sensitivity of trace gas abundances retrievals from infrared limb emission spectra to simplifying approximations in radiative transfer modelling, J. Quant. Spectrosc. Ra., 72, 249–280, https://doi.org/10.1016/S0022-4073(01)00123-6, 2002.

Thermodynamics Research Center, NIST Boulder Laboratories, Chris Muzny director, "Thermodynamics Source Database" in NIST Chemistry WebBook, NIST Standard Reference Database Number 69, Eds. P.J. Linstrom and W.G. Mallard, National Institute of Standards and Technology, Gaithersburg MD, 20899, https://doi.org/10.18434/T4D303, (retrieved January 29, 2025), 2025.

Trinkl, F.: Outflow from the Asian Summer Monsoon and Transport in the UTLS based on GLORIA Measurements during the PHILEAS Campaign 2023, Master thesis, Institute of Meteorology and Climate Research Atmospheric Trace Gases and Remote Sensing (IMKASF), Karlsruhe Institute of Technology (KIT), Karlsruhe, Germany, DOI: 10.5445/IR/1000186841, 2025.

Ungermann, J., Kleinert, A., Maucher, G., Bartolomé, I., Friedl-Vallon, F., Johansson, S., Krasauskas, L., and Neubert, T.: Quantification and mitigation of the instrument effects and uncertainties of the airborne limb imaging FTIR GLORIA, Atmos. Meas. Tech., 15, 2503–2530, https://doi.org/10.5194/amt-15-2503-2022, 2022.

Vasquez, K.: What's that Stuff?: Decaf coffee, C&EN, 2024, 102 (27), pp 22–23September 2, 2024.

Vogel, B., Günther, G., Müller, R., Grooß, J.-U., and Riese, M.: Impact of different Asian source regions on the composition of the Asian monsoon anticyclone and of the extratropical lowermost stratosphere, Atmos. Chem. Phys., 15, 13699–13716, https://doi.org/10.5194/acp-15-13699-2015, 2015.

Vogel, B., Volk, C. M., Wintel, J., Lauther, V., Clemens, J., Grooß, J.-U., Günther, G., Hoffmann, L., Laube, J. C., Müller, R., Ploeger, F., and Stroh, F.: Evaluation of vertical transport in ERA5 and ERA-Interim reanalysis using high-altitude aircraft measurements in the Asian summer monsoon 2017, Atmos. Chem. Phys., 24, 317–343, https://doi.org/10.5194/acp-24-317-2024, 2024.

https://doi.org/10.5194/egusphere-2026-3271
Preprint. Discussion started: 14 August 2026

Vogel, B., Lauther, V., Köllner, F., Ekinci, F., Rolf, C., Strobel, J., van Luijt, R., Volk, C. M., Borrmann, S., Dragoneas, A., Eppers, O., Molleker, S., Hoor, P., Ort, L., Weyland, F., Zahn, A., Clemens, J., Günther, G., Kachula, O., Müller, R., Ploeger, F., and Riese, M.: Continental and marine source regions contributing to the outflow of the Asian summer monsoon anticyclone during the PHILEAS campaign in summer 2023, Atmos. Chem. Phys., 26, 6283–6319, https://doi.org/10.5194/acp-26-6283-2026, 2026.

Wallington, T. J., Pivesso, B. P., Lira, A. M., Anderson, J. E., Nielsen, C. J., Andersen, N. H., and Hodnebrog, Ø.: CH_3Cl, CH_2Cl_2, $CHCl_3$, and CCl_4: Infrared spectra, radiative efficiencies, and global warming potentials, J. Quant. Spec. Rad. Trans., 174, 56–64, https://doi.org/10.1016/j.jqsrt.2016.01.029, 2016.

Wetzel, G., Kleinert, A., Johansson, S., Friedl-Vallon, F., Höpfner, M., Ungermann, J., Neubert, T., Catoire, V., Crevoisier, C., Engel, A., Gulde, T., Jacquet, P., Kirner, O., Kretschmer, E., Kulessa, T., Laube, J. C., Maucher, G., Nordmeyer, H., Piesch, C., Preusse, P., Retzlaff, M., Schardt, G., Schillings, J., Schneider, H., Schönfeld, A., Schuck, T., Woiwode, W., Riese, M., and Braesicke, P.: Intercomparison and validation of first GLORIA-B measurements of stratospheric and upper tropospheric long-lived tracers and photochemically active species, Atmos. Meas. Tech., 18, 5873–5894, https://doi.org/10.5194/amt-18-5873-2025, 2025.

Woiwode, W., Dörnbrack, A., Bramberger, M., Friedl-Vallon, F., Haenel, F., Höpfner, M., Johansson, S., Kretschmer, E., Krisch, I., Latzko, T., Oelhaf, H., Orphal, J., Preusse, P., Sinnhuber, B.-M., and Ungermann, J.: Mesoscale fine structure of a tropopause fold over mountains, Atmos. Chem. Phys., 18, 15643–15667, https://doi.org/10.5194/acp-18-15643-2018, 2018.